INFORMATION TO USERS

This manuscript has been reproduced from the microfilm master. UMI films the text directly from the original or copy submitted. Thus, some thesis and dissertation copies are in typewriter face, while others may be from any type of computer printer.

The quality of this reproduction is dependent upon the quality of the copy submitted. Broken or indistinct print, colored or poor quality illustrations and photographs, print bleedthrough, substandard margins, and improper alignment can adversely affect reproduction.

In the unlikely event that the author did not send UMI a complete manuscript and there are missing pages, these will be noted. Also, if unauthorized copyright material had to be removed, a note will indicate the deletion.

Oversize materials (e.g., maps, drawings, charts) are reproduced by sectioning the original, beginning at the upper left-hand corner and continuing from left to right in equal sections with small overlaps.

Photographs included in the original manuscript have been reproduced xerographically in this copy. Higher quality 6" x 9" black and white photographic prints are available for any photographs or illustrations appearing in this copy for an additional charge. Contact UMI directly to order.

Bell & Howell Information and Learning
300 North Zeeb Road, Ann Arbor, MI 48106-1346 USA
800-521-0600

The Effects of Elevated Mitochondrial Hydrogen Peroxide in *S. cerevisiae*: A Physiological Role for Cytochrome *c* Peroxidase

Tyrone Shephard

A Thesis

in

The Department

of

Chemistry and Biochemistry

Presented in Partial Fulfillment of the Requirements

for the Degree of Master of Science at

Concordia University

Montreal, Quebec, Canada

December 1999

ABSTRACT

The Effects of Elevated Mitochondrial Hydrogen Peroxide in *S. cerevisiae*: A Physiological Role for Cytochrome *c* Peroxidase

Tyrone Shephard

The role of cytochrome *c* peroxidase (CCP), found in yeasts and some bacteria, is not clear. However, it is believed to play a role in H_2O_2 detoxification. To probe the physiological role of CCP, a yeast strain deficient in the gene encoding CCP (Δ*ccp1*) was engineered and characterized with respect to growth on various carbon sources, respiratory competence, resistance to H_2O_2, activities of various antioxidant enzymes, and levels of glutathione. Mitochondria of Δ*ccp1* yeast were found to undergo time-dependent inactivation and the Δ*ccp1* strain was found to be more susceptible to H_2O_2-induced stress, as compared to the isogenic wild-type strain, during both its exponential and stationary phases of growth. Despite this increased sensitivity to H_2O_2, Δ*ccp1* was still able to adapt to stress. Furthermore, antioxidant enzymes such as glutathione reductase and catalase as well as the antioxidant glutathione, which are all regulated through the transcription factor YAP1, showed reduced activity in the Δ*ccp1* strain compared to the isogenic wild-type strain, possibly explaining the increased sensitivity of Δ*ccp1* cells to H_2O_2. The Δ*ccp1* strain also showed decreased phosphatase and increased kinase activities. These results suggest that CCP is involved in protecting mitochondria from H_2O_2 generated through normal metabolic reactions as well as from exogenous H_2O_2 challenges. They also indicate that CCP and/or H_2O_2 are involved in signal transduction in yeast. The creation of a yeast strain deficient in thioredoxin peroxidase (Δ*tsa1*), and its possible involvement in redox signaling, is also discussed.

ACKNOWLEDGEMENTS

I would like to acknowledge first and foremost Dr. Ann English for the support, encouragement and wisdom she gave me throughout my degree, and for making me a better researcher.

Secondly, I would like to express my gratitude to (i) Dr. Pam Hanic-Joyce and the members of my committee, Drs. Paul Joyce and Reginald Storms, who were always available and more than willing to provide me with help and guidance, (ii) my fellow lab members, Andrea Romeo, Lucile Serfass, Angelo Filosa, Christina Esposito, John Wright, Iolie Bakas, Dave Michaels, Susan Aitken and Robert Papp, who are all great people and great scientists, and who made my time spent in the lab enjoyable, (iii) my brother, Kyle, who despite a hectic schedule, was always willing to listen or talk with me about my research, and (iv) my girlfriend, Analia Barroetavena, for sometimes, undeservedly, taking second place to my research.

Finally, I would like to thank my parents for all the support and encouragement they have given me always.

TABLE OF CONTENTS

LIST OF FIGURES

LIST OF TABLES

CHAPTER 1

GENERAL INTRODUCTION

1.0 Introduction

The goals of this thesis are to determine the physiological role of cytochrome *c* peroxidase (CCP) and the effect of elevated mitochondrial hydrogen peroxide in yeast, *Saccharomyces cerevisiae*.

Although CCP has been widely studied (a PubMed query using "CCP" as a search term reveals 21560 entries), few experiments have been performed to determine its physiological role in yeast. Due to its ability to eliminate hydrogen peroxide (Reaction 1), CCP is believed to play a role in protecting yeast cells from H_2O_2-induced stress, yet experiments demonstrating clear evidence for this are lacking. To probe the physiological role of CCP, a yeast strain deficient in the gene encoding CCP, *CCP1*, was engineered (Δ*ccp1*) and characterized under normal growth conditions and in response to H_2O_2-induced stress. As CCP is a mitochondrial enzyme shown to eliminate up to 53% of H_2O_2 generated at the level of the mitochondrial respiratory chain (1), the Δ*ccp1* yeast strain also offered the opportunity to examine the effects of elevated mitochondrial hydrogen peroxide which, in humans, results in mitochondrial damage and is linked to apoptosis, aging and a number of degenerative diseases (18,39). Despite this link, there seem to be few *in vivo* models which demonstrate that physiologically generated levels of H_2O_2, in the absence of mitochondrial protective enzymes, actually damage mitochondria.

The Δ*ccp1* yeast strain also offered the opportunity to explore the putative role of H_2O_2 in cell signaling. Therefore, both mitochondrial integrity and signaling cascades were investigated in the Δ*ccp1* strain.

The results of the present investigations show *Δccp1* yeast to display (i) altered growth, (ii) decreased mitochondrial function with time, (iii) increased sensitivity to H_2O_2-induced stress, (iv) lower activity of catalase and glutathione reductase (GLR) during the stationary phase of growth, (v) lower glutathione levels, (vi) increased protein kinase A (PKA) acitvity and (vii) decreased phosphatase activity, relative to its isogenic wild-type.

This introduction will briefly review the current relevant known literature on (i) CCP, (ii) mitochondrial function, (iii) the growth of yeast, (iv) the cellular generation and removal of reactive oxygen species (ROS) as well as the damage and diseases reportedly caused by ROS, (v) signal transduction in yeast and (vi) H_2O_2-induced signaling.

1.1 CCP

CCP was discovered in and purified from baker's yeast in 1941 (2). It is a heme-containing enzyme that effectively catalyzes the oxidation of ferrocytochrome *c* ($cytc^{II}$) to ferricytochrome *c* ($cytc^{III}$) by H_2O_2 (3):

$$2cytc^{II} + H_2O_2 + 2H^+ \rightarrow 2\ cytc^{III} + 2\ H_2O \quad \text{(reaction 1)}$$

CCP is found in the mitochondria of aerobically grown yeast (4,5), the periplasmic space of some bacteria (6) and in the trematodes, *Fasciola hepatica* and *Schistosoma mansoni* (7). It has not been found in vertebrates and its exact physiological function in lower multicellular organisms is not known (7,8).

The location of CCP in *S. cerevisiae* is in the intermembrane space of the mitochondrion (9). This is appropriate as CCP is specific for ferrocytochrome *c*, also in the intermembrane space of the mitochondria, as an electron donor (10). Electrons from ferrocytochrome *c* results in the reduction of H_2O_2 through the direct use of electrons from the electron transport chain (ETC). The effects of CCP turnover on energy production are such that in the presence of excess H_2O_2, instead of fueling ATP production, electrons are used to detoxify H_2O_2 resulting in reduced levels of ATP (10).

The gene encoding CCP, *CCP1*, resides in the nucleus and is not part of the mitochondrial genome. Therefore, upon translation CCP resides in the cytosol where, in anaerobically growing yeast cells, it is present only as the apoenzyme (4). The holoenzyme is formed upon exposure of these cells to oxygen, which induces the insertion of a heme moiety into the apoenzyme and the translocation of CCP into mitochondria. The characteristic property of holoenzyme formation in the presence of oxygen is referred to as "induced conversion" (4,7,11).

Once active, Boveris has demonstrated that yeast CCP utilizes 53-55% of the H_2O_2 generated at the level of the mitochondrial respiratory chain thus preventing H_2O_2 leakage into the cytosol (1). CCP's ability to eliminate H_2O_2 has resulted in the belief by some researchers that its physiological function is protection against oxidative stress. However, a comparison of the $Km_{for\ HOOH}$ and $kcat_{for\ HOOH}$ values of CCP with those of the well-known protective enzyme, catalase, would seem to suggest that this is not so. CCP's $Km_{for\ HOOH}$ and $kcat_{for\ HOOH}$ values are 2.5×10^{-5} M and 1.4×10^{4} s^{-1} (12), respectively, while catalase has $Km_{for\ HOOH}$ and $kcat_{for\ HOOH}$ values of 2.5×10^{-2} M and 1×10^{7} s^{-1} (13), respectively. A comparison of the kcat values reveals that CCP is 10^3 times slower at

eliminating H_2O_2 compared to catalase at high H_2O_2 concentrations, an undesirable property if CCP is a protective enzyme. Despite its relatively low kcat, there is research showing that CCP does protect against oxidative stress. Campos et al. (7) have reported that *Fasciola hepatica* CCP can protect deoxyribose from oxidative damage *in vitro* and speculate that this protection is due to the prevention of $^{\bullet}OH$ radical formation from H_2O_2 by Fenton reactions. Furthermore, the activity of CCP is increased, likely due to the transcriptional activating protein Yap1p (14), in yeast strains containing elevated levels of intracellular H_2O_2. (15,16). Δ*ccp1* yeast strains also show increased sensitivity, when compared to isogenic wild-type cells, to the lethal effects of heat (believed to involve oxidative stress) (17).

1.2 Yeast Mitochondria

In order to understand how CCP might be involved in, or if its elimination affects, mitochondrial function, it is necessary to first understand how mitochondria function. Mitochondria are compartmentalized organelles that contain both an outer and inner membrane (Figure 1.1). The space between the outer and inner membrane is referred to as the intermembrane space, while the space enclosed by the inner membrane is termed the matrix. Mitochondria are unique in that they are the only other organelle in yeast, beside the nucleus, to contain DNA. Yeast mitochondrial DNA (mtDNA) is attached to the inner mitochondrial membrane, inside the matrix, and lacks introns and histones (18). This lack of introns and histones, as well as the lack of a complete proofreading mechanism, results in mtDNA being especially susceptible to ROS induced damage (18).

However, mtDNA is protected by antioxidant enzymes such as SOD, GLR and glutathione peroxidase [debated to be present in *S. cerevisiae* (15)], which occupy the mitochondrial matrix (19). Yeast mtDNA encodes many critical catalytic subunits for NADH dehydrogenase (complex I), ubiquinol cytochrome *c* reductase (complex III), cytochrome *c* oxidase (complex IV) and ATP synthase (complex V), all of which are members of the ETC (20). When yeast cells undergo damage to their mtDNA they are often unable to carry out mitochondrial ATP synthesis. These cells are, however, still viable due to their ability to generate ATP derived from glycolysis. Yeast cells with damaged mtDNA resulting in nonfunctional mitochondria are commonly referred to as petite (due to the small size they display on YPDG plates) or $[rho]^-$ cells. Yeast cells with no mtDNA are labeled $[rho]^0$ cells.

The main function of mitochondria is the production of energy in the form of ATP. However, mitochondria are also responsible for Ca^{2+} storage, and oxidation of a variety of substrates including pyruvate, ketone bodies, amino acids and fatty acids (19). Production of ATP requires 1) a flow of electrons through the ETC and 2) a flow of H^+ ions through complex V (Figure 1.1) (19). Electrons are provided to the iron sulfur centers of complex 1 and succinate dehydrogenase (complex 2) from NADH and succinate, respectively (Figure 1.1), and passed on to co-enzyme Q. Co-enzyme Q then passes these electrons to complex III, which reduces cytochrome *c*. The electrons transferred to cytochrome *c* can be used by CCP to reduce H_2O_2 or, more commonly, are transferred to complex IV which uses them, in addition to two H^+ ions, to reduce O_2 to H_2O. During this process of electron transport an electrochemical gradient is formed through the pumping of protons by complexes I, III and IV from the matrix into the

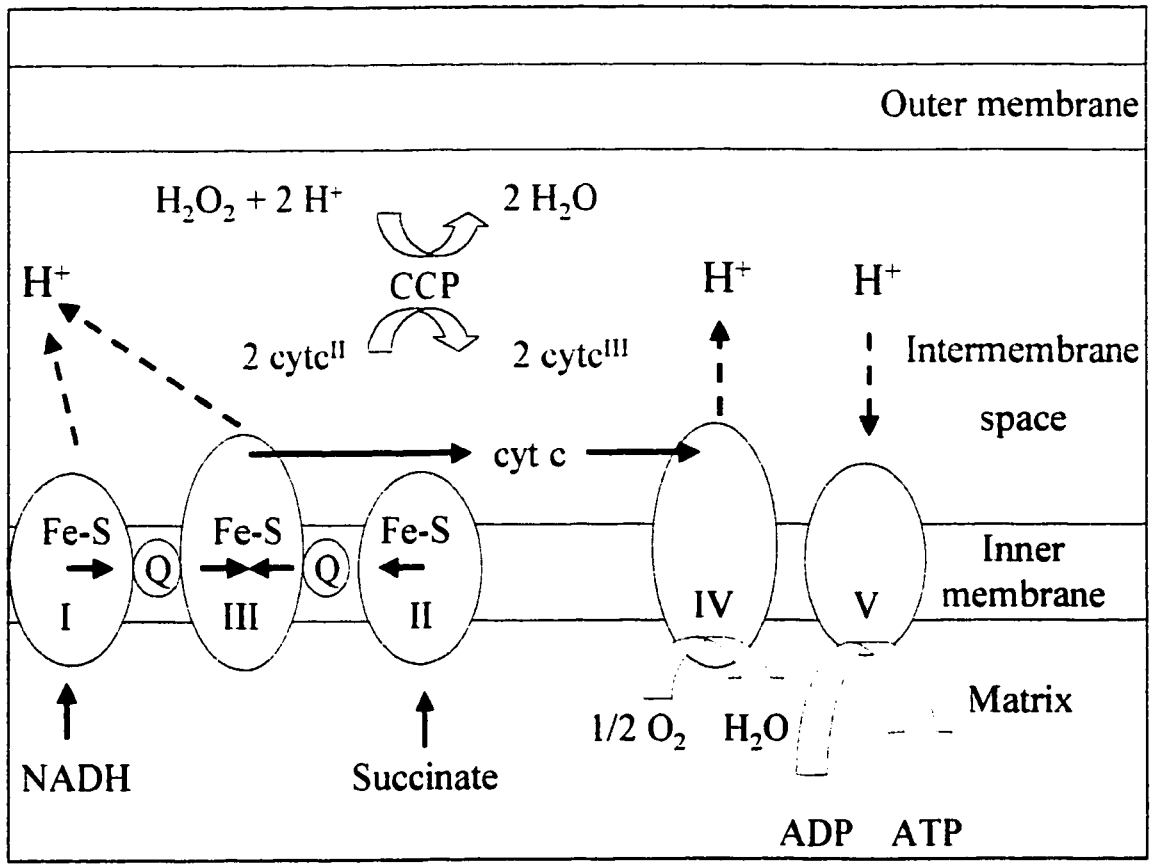

Figure 1.1 Oxidative phosphorylation in yeast mitochondria. The electron transport proteins (complex I-IV) and the ATP synthase (complex V) are shown in their probable orientation in the mitochondrial inner membrane. The lipid-soluble electron shuttle, co-enzyme Q, is depicted as Q. The flow of electrons is indicated by the solid black arrows, while dashed arrows indicate the flow of H^+ ions. This Figure is a modified version of Figure 2.2 in Reference 19.

intermembrane space. The transport of protons in the reverse direction through complex V is used to drive the synthesis of ATP.

The integrity of the members of the ETC located in the inner membrane, along with the integrity of the inner membrane itself, which maintains the proton gradient, is vital to the production of ATP (19). It might be hypothesized that the function of CCP, due to its location in the intermembrane space, is to protect the inner membrane and its components from H_2O_2-induced damage. This might be especially important due to the lack of other protective enzymes or antioxidants found in the intermembrane space (19).

1.3 Growth of Yeast

As mentioned before, yeast cells are somewhat unique in their ability to survive by either fermentation, which generates energy through the process of glycolysis, or respiration, which generates energy through the ETC (21). When cultivated in glucose rich medium (YPD), yeast grow first by fermentation when the carbon source is plentiful, and then later, as the carbon source becomes used up, by respiration. A normal yeast growth curve for cells grown in YPD exhibits five distinct stages following reproliferation of cells from stationary phase (stage in which cells have stopped replicating and are in a G_0 state). These include a lag phase, an exponential phase, the diauxic shift, the post-diauxic phase and stationary phase (Figure 1.2).

When stationary-phase cells are first placed in glucose rich media they exhibit a lag phase. Lag phase is defined as the time required for stationary-phase cells to re-enter the cell cycle and begin replicating. During the lag phase cells switch their metabolism from

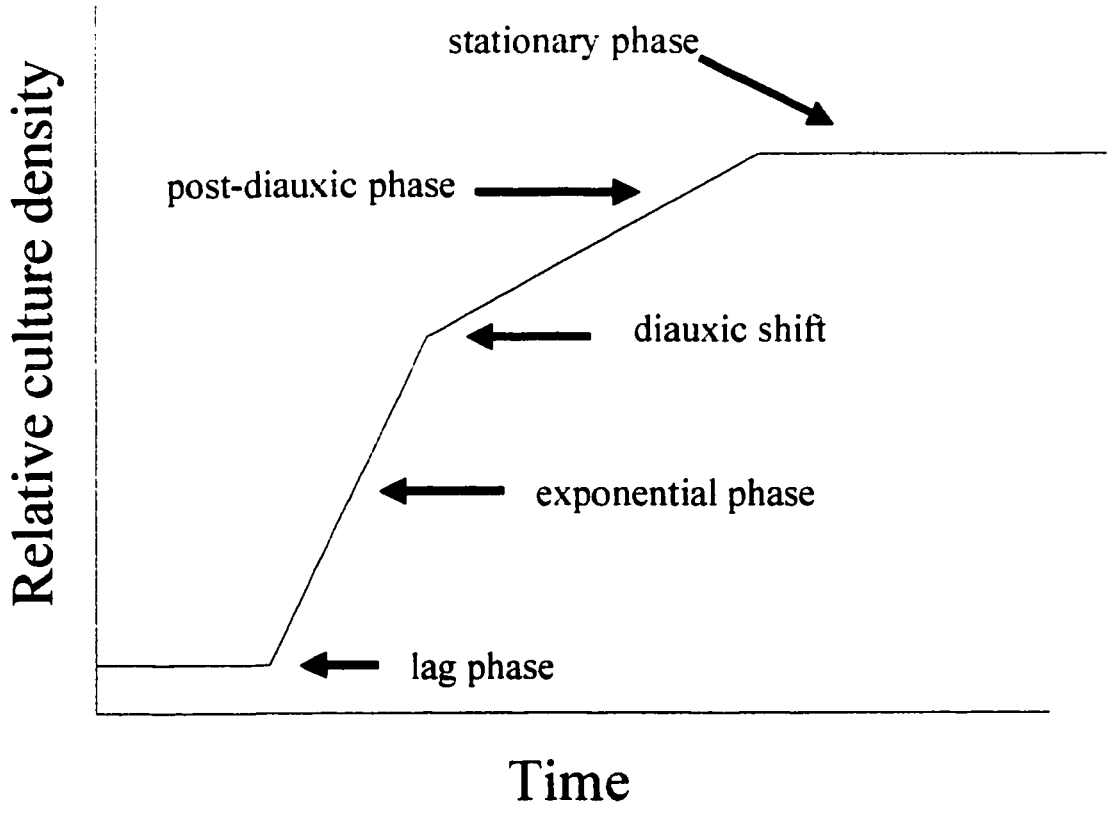

Figure 1.2 The growth curve displayed by yeast on a fermentable carbon source such as glucose. This diagram displays the five distinct stages of growth (lag phase, exponential phase, diauxic shift, post-diauxic phase, and stationary phase) exhibited by yeast when given a fermentable carbon source. Culture density is measured by turbidity at 600 nm. This diagram was taken from Werner-Washburne et al. (23).

a respiratory mode to a fermentative mode (22). In doing so, they down-regulate genes and enzymes involved in gluconeogenisis and respiration, and up-regulate genes and enzymes that function in glycolysis (22). Following the lag phase is the exponential phase. Exponential-phase cells have already up regulated all the necessary genes and enzymes required for glycolysis and exhibit rapid logarithmic growth. This glycolytic form of metabolism, and exponential growth, lasts indefinitely as long as there is enough fermentable sugar around to support it (22). Besides enzymes involved in respiration, antioxidant enzymes as well as enzymes involved in gluconeogenis are all down regulated in this growth phase.

As glucose levels start to diminish, yeast cells switch from fermentative-based growth to respiratory-based growth. The point at which this switch takes place is known as the diauxic-shift (23). At this point, the rate of protein synthesis decreases but recovers partially during the post-diauxic phase (23). However, despite a general decrease in protein synthesis, some proteins show increased synthesis. *CTT1* encoding cytosolic catalase is one of a group of 16 genes that are coordinately induced early in the diauxic shift (24). Other members of this group include *UBI4* encoding ubiquitin and *HSP12* encoding a heat shock protein (25). Since these proteins are involved in eliminating either oxidative stress or proteins damaged by oxidative stress, their induction would seem to indicate that respiration generates a lot of oxidative stress.

After switching to respiratory growth, cells enter a growth phase known as the post-diauxic phase (23). During this phase cells grow by respiration and utilize energy generated from the metabolism of ethanol (formed during fermentation) (26). This phase

is characterized by a decreased growth rate (26) and an increase in number of mitochondria (27).

Finally, due to starvation, yeast cells arrest growth and enter stationary phase (26). In stationary phase, yeast cells are synchronized such that the population is composed predominately of unbudded cells in the G_0 portion of the cell cycle (23). Entry into stationary phase is thought to be a highly regulated process that activates a program for long-term survival in the absence of cell division and without added nutrients (23). Energy in stationary phase is generated primarily by mitochondria, and metabolism is greatly reduced enabling cells to survive for weeks to months without additional nutrients (21). In addition to lowered metabolic rates, stationary-phase yeast cells also exhibit increased tolerance to oxidative stress and heat (21), as well as undergo physiological changes such as alterations in cell wall and chromatin structure, and accumulate the storage carbohydrates glycogen and trehalose (23,28). The increased tolerance to oxidative stress (29) displayed by stationary-phase cells can be explained by the up regulation of a number of antioxidant enzymes including catalase (28), GLR (26) and SOD (30). The up regulation of these enzymes is mediated, at least in part, by the c-jun related proteins Yap1p and Yap2p (29) (Section 1.5), which up regulate antioxidants such as GLR (26), and in part to the *ras*-adenylate cyclase pathway, which, through the action of protein kinase A, activates genes such as catalase through STRE elements (C_4T sequences contained in promoters) (Section 1.5).

In addition to growth on glucose, yeast cells can also be cultured in nonfermentable growth sources such as YPG or YPE, which contain glycerol and ethanol, respectively, as carbon sources. Yeast cells grown in the presence of nonfermentable carbon sources, are

forced to rely exclusively on respiration for energy production, and therefore do not exhibit many of the characteristics, such as decreased gluconeogenisis and rapid growth, associated with glucose stimulated exponential-phase growth (22).

1.4 Reactive Oxygen Species

The Generation of ROS

The term ROS is used to describe the following species: singlet oxygen, the superoxide anion radical ($O_2^{\bullet -}$), H_2O_2, lipid peroxides, nitric oxide (NO), peroxynitrite ($ONOO^-$), the thiyl peroxyl radical ($RSOO^{\bullet}$), the ferryl radical (FeO^{2+}) and the hydroxyl radical ($OH^{\bullet}$) (31). ROS are generated in cells by several pathways, and can be directly produced through UV- irradiation (Figure 1.3) (32).

The main sites of ROS generation *in vivo* are complexes I and III of the respiratory chain (33, 32, 1). Electron transport through the mitochondrial respiratory chain is extremely efficient, and normally the vast majority of O_2 is converted to H_2O_2. However, 1-2% of electrons leak out and generate the superoxide anion ($O_2^{\bullet -}$) in univalent reactions mediated by coenzyme Q and ubiquinone and its complexes (32). NADPH cytochrome P450 reductase, hypoxanthine/xanthine oxidase, NADPH oxidase, lipoxygenase and cyclooxygenase also generate $O_2^{\bullet -}$ (32).

H_2O_2 is created in the mitochondria at complexes I and III through the dismutation of $O_2^{\bullet -}$ by SOD (reaction 2), and as a product of monoamine oxidase (MAO) catalysis which is associated with the outer mitochondrial membrane. H_2O_2 is further generated through the β-oxidation of fatty acids (34), (35), through flavoproteins (36), and by the

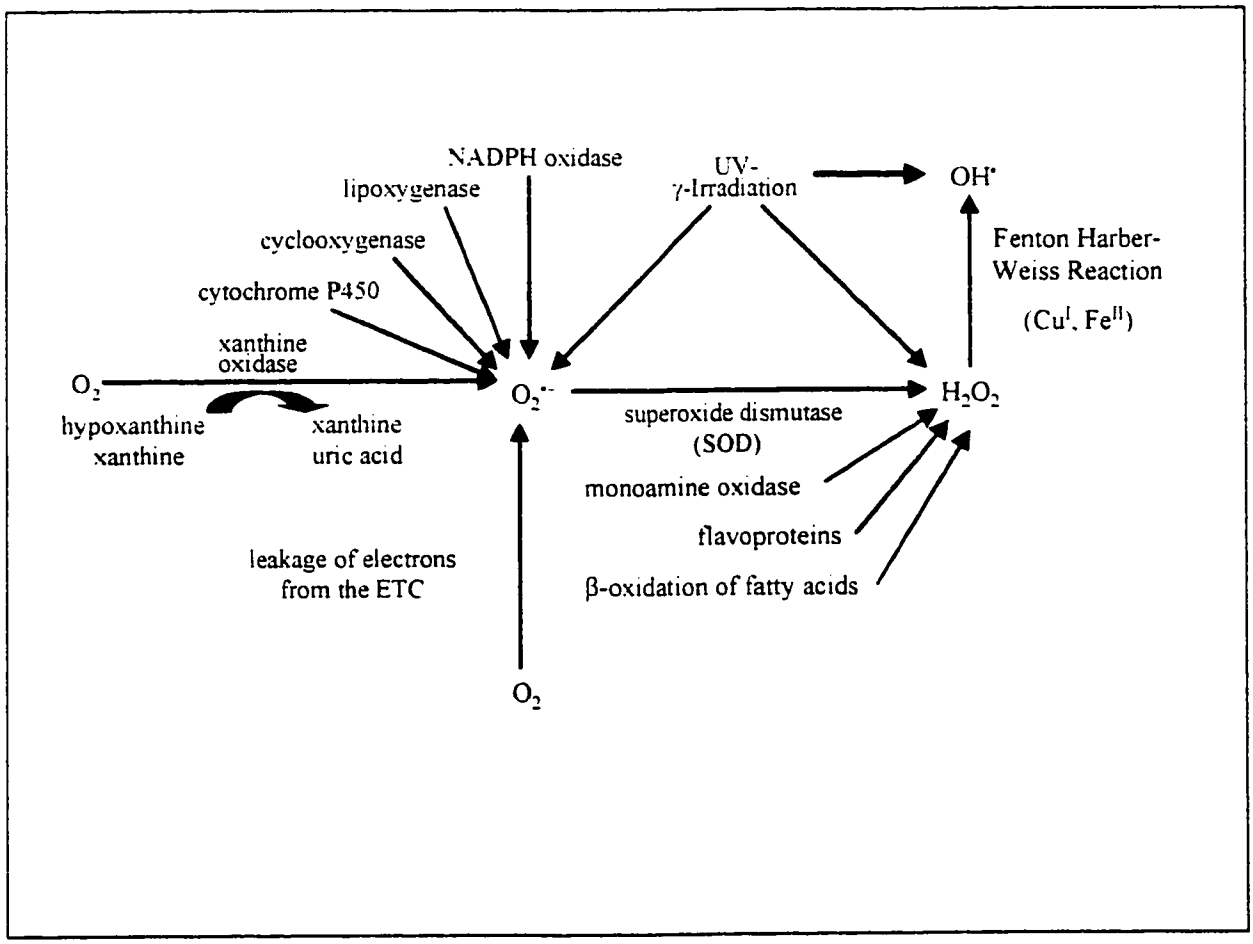

Figure 1.3 Metabolic pathways of reactive oxygen species. Reactive oxygen species such as H_2O_2, $O_2^{\bullet-}$ and $OH^{\bullet}$ are generated in cells by several pathways. $O_2^{\bullet-}$ is generated by the leakage of electrons from mitochondria, NADPH oxidase, cytochrome P450 reductase, hypoxanthine/xanthine oxidase, lipoxygenase and cyclooxygenase. SOD converts $O_2^{\bullet-}$ into H_2O_2, which is also created by monoamine oxidase, flavoproteins and the β-oxidation of fatty acids. H_2O_2 produces the highly reactive $OH^{\bullet}$ by the Fenton or Harber-Weiss reactions. This figure is a modified version of Figure 1 in Reference 32.

action of oxidases (reaction 3). H_2O_2 production is particularly high when mitochondria are in a resting condition, i.e., when the electrochemical proton gradient is high and respiration rate is limited by a lack of ADP (such as in stationary phase) (1,33). Under these conditions, it is postulated that the generation of mitochondrial H_2O_2 is up to 30% higher (1) generating a possibly dangerous source of $OH^{\bullet}$, especially if the antioxidant defences that eliminate H_2O_2 are not working.

In the presence of Fe^{II} or Cu^{I}, H_2O_2 can form the highly reactive $OH^{\bullet}$ radical through the Fenton reactions (reaction 4) (32). Mitochondria contain high levels of iron and copper (18) and thus, when H_2O_2 levels are not controlled, represent potentially dangerous sources of $OH^{\bullet}$ (18).

$2\ O_2^{\bullet-} + 2H^+ \rightarrow H_2O_2 + O_2$ (reaction 2)

$RH_2 + O_2 \rightarrow R + H_2O_2$ (reaction 3)

$H_2O_2 + Fe^{II}$ (or Cu^{I}) $\rightarrow OH^- + OH^{\bullet} + Fe^{III}$ (or Cu^{II}) (reaction 4)

Another potentially dangerous source of $OH^{\bullet}$ is the peroxynitrite anion $ONOO^-$ formed by the reaction of nitric oxide ($NO^{\bullet}$) with $O_2^{\bullet-}$. This highly reactive molecule supposedly breaks down to form $OH^{\bullet}$ and $NO_2^{\bullet}$ (reaction 5) (37). Interestingly, CCP has recently been shown in our lab (I. Bakas, unpublished observations) to be efficient in the elimination of peroxynitrite.

$NO^{\bullet} + O_2^{\bullet-} \rightarrow ONOO^- + H^+ \rightarrow ONOOH \rightarrow OH^{\bullet} + NO_2^{\bullet}$ (reaction 5)

Damage Induced by ROS

ROS are known to damage DNA, proteins and lipids, and are thought to lead to the damage of virtually every molecule (18). ROS damage DNA by initiating double-stranded breaks (18), single-stranded breaks, sugar damage and DNA-protein crosslinks (38). $OH^{\bullet}$, a likely byproduct of excess H_2O_2, modifies ribose phosphates and pyrimidine nucleosides and nucleotides, and reacts with the sugar phosphate backbone of DNA resulting in strand breaks. Hydroxylation of deoxyguanosine residues by $OH^{\bullet}$ produces 8-hydroxydeoxyguanosine (8OHG), which is used as a marker of oxidative DNA damage. This marker has been used in yeast to show that lethal concentrations of H_2O_2 cause DNA damage, likely through formation of $OH^{\bullet}$ radicals (38).

Oxidative damage to proteins involves oxidation of the amino acids His, Arg, Lys, Pro, Met and Cys, which can render proteins structurally or catalytically inactive (38). ROS also result in protein crosslinking, which leads to the increased proteolytic susceptibility and decreased biological activity of the proteins involved (38). Again it appears to be the hydroxyl radical, and to a lesser extent other ROS, that cause protein damage (18). Because of the high protein content of the inner mitochondrial membrane (75%), it is expected that these proteins are one of the primary targets of mitochondrially generated ROS. Furthermore, it is believed that cysteine residue oxidation results in mitochondrial dysfunction (18).

ROS also damage membranes through the oxidation of fatty acids, which results in their decreased fluidity and increased permeability, and eventually cell death. Lipid

peroxidation of membranes is initiated by a free radical which abstracts a hydrogen atom from unsaturated fatty acids leading to the generation of lipid radicals (18). End products of lipid peroxidation, such as epoxides, aldehydes and alkanes are also known to damage DNA and inactivate proteins (38). Yeast, when challenged with H_2O_2, show signs of lipid peroxidation as displayed by increased malondialdehyde formation which is directly related to the degree of unsaturation of fatty acids present in a membrane (38).

Lipid peroxidation could be particularly high in mitochondria due to the mitochondrial accumulation of low molecular weight Fe^{2+}complexes (39). As well, cardiolipin, a major component of the inner mitochondrial membrane, is decreased to a larger extent than other lipids upon exposure to oxidative stress (39) which is thought to be due to its high unsaturation (39). Cardiolipin oxidation is especially harmful as this lipid is required for the activity of cytochrome oxidase and other mitochondrial proteins (39). Mitochondrial-membrane lipid peroxidation results in irreversible loss of mitochondrial functions such as oxidative phosphorylation and ion transport (18).

Pathologies Associated with ROS

There is almost no area in human pathology where oxidative stress has not been implicated (39). Mitochondrial malfunction due to oxidative stress has been associated with diseases such as Parkinson's and Alzheimer's as well as with aging and apoptosis.

For example affected brain areas of patients with Alzheimer's disease exhibit an increased production of 8OHG from mtDNA compared to age-paired controls (39). In Parkinson's disease, severe compromissions of complex I, as well as lowered levels of glutathione, have been found in the substantia nigra of victims. Both these observations

implicate mitochondrial malfuction and oxidative stress in the onset of Parkinson's disease (39).

Accumulation of somatic mutations of mtDNA with age has led to the mitochondrial theory of aging. This theory proposes that a vicious circle is established involving mtDNA damage, altered oxidative phosphorylation and overproduction of ROS (39). As mentioned previously, mtDNA is extremely susceptible to oxidative damage as it lacks introns and is devoid of histones. Furthermore, its location in the matrix places it very close to the ETC, the major source of ROS in the cell. It has been shown that the 8OHG content of mtDNA is increased in aging and age-associated diseases (39). The theory that mitochondrial ROS are responsible for aging is further supported by the finding that decreased caloric intake in rodents, which is accompanied by decreased state 4 respiration and thus decreased superoxide production, results in increased longevity, also increased expression of mtSOD and catalase in Drosophila result in increased life span (39).

Mitochondrial dysfunction caused by ROS is attributed to both accidental cell death (necrosis) and programmed cell death (apoptosis) (18). Necrosis occurs when a cell is submitted to a damaging situation severe enough to cause irreversible dysfunction of essential cellular components. Apoptosis is a form of programmed cell death that occurs even when there is no irreversible damage to cellular components. This process is physiological and necessary for maintenance of life in multicellular organisms since it eliminates unnecessary cells. Ineffective induction of apoptosis may lead to diseases such as cancers and autoimmune disorders. Apoptosis occurs after the activation of an intrinsic cell-suicide program. One of the first steps in this suicide program is a decrease in

mitochondrial membrane potential, which results in the release of cytochrome *c* and/or apoptosis inducing factor (AIF) from the intermembrane space of the mitochondria (20). Released cytochrome *c* then goes on to activate caspases, a family of proteases that are established apoptotic executioners and responsible for the morphological hallmarks of apoptosis, including cell shrinkage, membrane blebbing and chromatin degradation (20).

ROS in mitochondria are thought to induce apoptosis by oxidizing pyridine nucleotides which enhance Ca^{2+} efflux from mitochondria. Reuptake of released Ca^{2+} by mitochondria (Ca^{2+} cycling) induces a nonspecific inner membrane permeabilization referred to as mitochondrial permeability transition (MPT) (18,86). This permeabilization is dependent on the presence of intramitochondrial Ca^{2+} and is reversed by Ca^{2+} chelators (18). With the membrane permeable, cytochrome *c* is released and apoptosis is initiated (18). Proof that ROS are involved in the MPT is demonstrated by experiments showing that catalase inhibits calcium-induced MPT (18).

In addition to multicellular organisms, apoptosis has been shown to occur in *S. cerevisiae*. Apoptosis in unicellular cells is thought to offer an evolutionary advantage by eliminating cells damaged by ROS that might produce either no or impaired offspring. This suicidal death is reasoned to be for the good of the colony, as damaged cells would consume resources otherwise available to healthy cells. Apoptosis in *S. cerevisiae* occurs when cells are depleted of glutathione or challenged with low levels of H_2O_2 (3 mM), as opposed to high levels (180 mM), which results in necrosis, (40). Apoptotic cell death in *S. cerevisiae* is thought to be due to an accumulation of oxygen radicals, as it was determined that oxygen radical scavengers or hypoxia prevented the apoptotic death of these cells (40).

Defences to inactivate ROS

Now that links between oxidative damage, various disease states and aging are firmly established, there is a rapidly expanding interest in the systems that protect against ROS in the eukaryotic cell. Due to its relative simplicity, yeast may provide an important tool to study these mechanisms. In order to maintain ROS at physiologically unharmful levels, yeast cells possess both enzymatic, and non-enzymatic, primary and secondary antioxidant defence systems. Primary defences operate to neutralize ROS while secondary defences repair or remove the products of oxidation damage to DNA, proteins and lipids (38).

There is evidence that, in yeast, oxidatively modified proteins are substrates for the ubiquitination system for intracellular protein turnover. This is supported by the finding that inactivation of the polyubiquitin gene (*UBI4*) increases the sensitivity of yeast to H_2O_2-induced inactivation (38). Another important secondary defense protein is activating protein (AP) nuclease, encoded by the *APN1* gene, which is implicated in the repair of ROS-induced DNA damage in yeast. This was demonstrated by findings showing that *APN1* mutants are hypersensitive to H_2O_2. The primary antioxidant defense systems in yeast, their functions and, where known, the transcription factor that induces them, are listed in Table 1.1 These primary antioxidants and antioxidant enzymes will now be discussed in greater detail.

1. Glutathione

Of the nonenzymic defences, glutathione is particularly important as a free-radical scavenger. Its redox active sulphydryl group enables it to react directly with oxidants, eliminating ROS and generating oxidized glutathione (GSSG) in the process:

$2\,GSH \rightarrow GSSG + 2e^{-} + 2H^{+}$ (reaction 6)

Table 1.1 Yeast Primary Antioxidant Defences*.

Genes (product)	Function	Regulation by:
SOD1 (CuZnSOD; cytoplasmic)	Dismutation of superoxide anion	Yap1p
SOD2 (MnSOD; mitochondrial)	Dismutation of superoxide anion	Yap1p
CTA1 (catalase A; peroxisomal)	Decomposition of hydrogen peroxide	Negatively regulated by PKA
CTT1 (catalase T; cytoplasmic)	Decomposition of hydrogen peroxide	Negatively regulated by PKA
CCP1 (cytochrome *c* peroxidase)	Reduction of hydrogen peroxide	Yap1p
GSH1 (γ-glutamylcysteine synthetase)	Reduction of protein disulfides; scavenging of free radicals; conjugation with electrophilic substrates; binding of Cd	Yap1p
GLR1 (GLR)	Reduction of oxidized glutathione	Yap1p
ZWF (glucose-6-phosphate dehydrogenase)	Reduction of $NADP^{+}$ to NADPH	Yap1p
CUP1 (metallothionein)	Binding of Cu, preventing the Fenton reaction; scavenging of superoxide and hydroxyl radicals (?)	
TRX2 (thioredoxin) *TSA1* (thioredoxin peroxidase)	Reduction of protein disulfides reduction of hydrogen peroxide and alkyl hydroperoxides	Yap1p
SPE2 (polyamines)	Protection of lipids from oxidation	

*This table was taken from Moradas-Ferreira et al. (38).

Lack of glutathione in animals has been shown to lead to several diseases associated with damaged mitochondria. Damage is believed to occur due to a buildup of H_2O_2

which can usually, in the presence of reduced glutathione, be removed by mitochondrial glutathione peroxidase (41). However, since glutathione peroxidase removes H_2O_2 by oxidizing reduced glutathione, the elimination of glutathione results in loss of glutathione peroxidase activity (41). It is still not clear as to whether or not glutathione peroxidase exists in *S. cerevisiae* (15).

S. cerevisiae strains deficient in glutathione synthesis (*Δgsh1)* are viable but have slower growth rates and cannot grow by respiration (38). Cells deficient in glutathione synthesis are also more susceptible to H_2O_2-induced stress, compared to isogenic wild-type cells, in both exponential- (41,42) and stationary-phase growth (1 day of growth in the reported experiment) (42). Despite their susceptibility to H_2O_2-induced stress, *GSH1* mutants are still able to elicit an adaptive response to H_2O_2 (i.e., they show resistance to lethal concentrations of H_2O_2 when pretreated with sublethal concentrations), indicating that other protective mechanisms are available to be up regulated for elimination of H_2O_2-induced stress (42). Also interesting, are the apoptotic signs exhibited by the *ΔGSH1* mutants when incubated in a glutathione-free medium. In this medium *ΔGSH1*-mutant cells display DNA fragmentation, condensation of chromatin and exposition of phosphatidylserine at the outer leaflet of the plasma membrane, which are all charactristic signs of apoptosis (40). Increased glutathione levels both upon exposure to H_2O_2-induced stress and upon entry into stationary phase are mediated by Yap1p (43).

2. Superoxide dismutase

SOD eliminates reactive $O_2^{\bullet-}$ by dismutating it to H_2O_2 and O_2 (reaction 2). SOD exists in two forms in both mammalian and yeast cells. These include a mitochondrial

manganese-containing enzyme (MnSOD), encoded by *SOD2* in yeast, and a cytoplasmic copper/zinc-containing enzyme (CuZnSOD), encoded by *SOD1* in yeast (44). In yeast, MnSOD acounts for 1 to 10% of the total SOD activity depending on the growth conditions, while cytoplasmic CuZnSOD accounts for the rest (21). The transcription of *SOD2* increases 6.5-fold upon entry into stationary phase, compared to exponential phase, and again increases under conditions of hyperoxia or $O_2^{\bullet-}$ stress (46), demonstrating its importance under respiratory conditions. Both SOD enzymes have been shown to be important in yeast for the removal of $O_2^{\bullet-}$ generated during the course of normal metabolism and that produced from redox-cycling compounds such as menadione and plumbagin (44). More recently, it has been shown that both *SOD1* and *SOD2* are induced by Yap1p in response to oxidative stress (14).

The removal of either *SOD1* or *SOD2* results in decreased growth of yeast under high aeration (hyperoxia), while yeast strains deficient in both *SOD1* and *SOD2* fail to grow (44). Results showing that low aeration or removal of respiration, via a secondary mutation, dramatically increases the survival of these yeast strains under hyperoxia provide proof that respiration is at least partly responsible for the initial damage (44). Experiments on *SOD2* mutants show that mitochondrial components are the primary targets of $O_2^{\bullet-}$ produced at intramitochondrial sites and that without *SOD2* mitochondria undergo time-dependent damage that eventually prevents their proper function. It was concluded that this damage was primarily inflicted on mitochondrial proteins and membranes and that mtDNA damage was secondary (21).

3. Catalase

Catalase removes hydrogen peroxide by a disproportionation reaction that converts it into water and oxygen:

$2\ H_2O_2 \rightarrow 2\ H_2O + O_2$ (reaction 7)

S. cerevisiae contains two catalases, peroxisomal catalase (catalase A) and cytosolic catalase (catalase T), encoded by the *CTA1* and *CTT1* genes, respectively (41). *CTT1* transcription and catalase activity are increased in response to exogenous H_2O_2 stimulation (45) (14), and the increased transcription has recently been shown to be dependent on Yap1p (14). *CTT1* transcription is also controlled by the *ras*-adenylate cyclase pathway due to the presence of stress response elements (STRE's) contained in its promoter. *CTT1* increases its transcription in stationary-phase and in response to heat shock (17) through this STRE element (38), which, in addition to Yap1p, is also involved in increasing *CTT1* expression in response to H_2O_2-induced stress (38). Induction of *CTT1* through the STRE element is linked to PKA activity (PKA is a member of the *ras*-adenylate cyclase pathway), as catalase activity is enhanced in *ras2* mutant strains (which have low PKA activity) and prevented in *BCY1* mutant strains (which exhibit high constitutive PKA activity) (38). Yeast strains deficient in either *CTT1* or *CTA1* are unable to elicit an adaptive response to H_2O_2 and are mildly susceptible to H_2O_2-induced stress in stationary phase. Yeast strains deficient in both *CTT1* and *CTA1* are also unable to adapt to H_2O_2-induced stress and are highly susceptible to H_2O_2-induced stress during stationary phase (41).

4. Glutathione reductase

GLR is a flavoenzyme, which catalyzes the reduction of GSSG to GSH using the reducing power of NADPH (25):

$$GSSG + 2e^- + NADPH^+ + H^+ \rightarrow 2GSH + NADP^+ \quad \text{(reaction 8)}$$

GLR is needed to maintain the high intracellular ratio of GSH to GSSG so that the cell maintains a reducing environment. Yeast mutants deleted for the gene encoding GLR (*GLR1*) demonstrate normal growth, but, exhibit increased sensitivity to oxidants, including both peroxides and $O_2^{\bullet -}$ (26). This indicates a requirement for GLR in protection against oxidative stress (25). Δ*glr1* yeast mutants show only slightly increased susceptibility to H_2O_2-induced stress during their exponential phase of growth but are much more susceptible during stationary phase, where they exhibit 50% survival compared to isogenic wild-type cells when challenged with 12 mM H_2O_2 (26). Furthermore, *GLR1* expression is elevated 2- to 3-fold in the presence of oxidants. This H_2O_2-mediated induction as well as its 3- to 4-fold stationary-phase induction is dependent on the Yap1p transcriptional activator protein (14,26). Similar to Δ*gsh1* mutants, Δ*glr1* mutants are unaffected in their inducible adaptive response to H_2O_2 (25), again suggesting the involvement of other protective mechanisms. Δ*GLR1* mutants also accumulate oxidized glutathione and possesses a 2-fold increase in total glutathione (46). It is also interesting to note that strains lacking functional mitochondria do not

demonstrate the characteristic stationary-phase increase in GLR activity (26) implicating mitochondrial control of GLR activity.

5. Thioredoxin peroxidase

Thioredoxin peroxidase removes H_2O_2 using either thiols (RSH) or the NADPH-dependent thioredoxin system as electron donors:

$H_2O_2 + 2RSH \rightarrow RSSR + 2\ H_2O$ (reaction 9)

Yeast strains deficient in the gene encoding thioredoxin peroxidase (*TSA1*) show no difference in phenotype under normal growth conditions, but in the presence of H_2O_2 exhibit slower growth under aerobic conditions (47). Furthermore, thioredoxin peroxidase protein levels increase 3-fold when cells are shifted from an anaerobic to a hyperaerobic environment (46). This would seem to indicate that thioredoxin peroxidase is important under aerobic conditions where yeast cells are subjected to oxidative stress.

Δ*tsa1* yeast strains also display increased sensitivity to oxidative stress induced by *tert*-butylhydroperoxide, H_2O_2, cumene hydroperoxide, and menadione (46) (48). Furthermore, the transcription of *TSA1* is also induced by Yap1p in response to oxidative stress (14). Finally, thioredoxin peroxidase has been shown to protect cells from the lethal effect of heat exposure by decreasing the steady-state level of intracellular oxidants (46).

6. Glucose-6-phosphate dehydrogenase

Glucose-6-phosphate dehydrogenase catalyzes the oxidation of glucose-6-phosphate to 6-phosphogluconolactone, and is a key enzyme in the generation of NADPH via the pentose phosphate cycle (15). NADPH is important in maintaining the reducing environment of the cell as it is required by GLR to maintain reduced levels of glutathione (reaction 8) (38). NADPH is also found bound to catalase and required to maintain its active form (26). Yeast cells containing mutations in *ZWF1*, which codes for glucose-6-phosphate dehydrogenase, exhibit normal growth but also increased sensitivity to H_2O_2 in exponential phase. Furthermore, they cannot adapt to H_2O_2-induced stress (38) indicating that NADPH synthesis via the pentose phosphate pathway is a key step in H_2O_2 decomposition. *ZWF1* is also induced by Yap1p in response to H_2O_2, while it is repressed by methionine and S-adenosylmethionine (46).

7. Mitochondria

There is evidence that, despite their production of free radicals, mitochondria themselves are involved in protection against oxidative stress. Jamieson has shown that a $[rho]^-$ strain is more susceptible to H_2O_2-induced stress in exponential phase and after 24 hours (which he labels stationary phase) (27). Furthermore, Grant et al. have shown that $[rho]^0$ mutants and strains deleted for the nuclear genes *COX6* and *COX3*, which are required for the function of the ETC, are more sensitive to H_2O_2 (49). They further demonstrate that treatment of isogenic wild-type cells with the mitochondrial respiratory inhibitors antimycin A, oligomycin, potassium cyanide and sodium azide, increases the

sensitivity of these cells to H_2O_2. Due to the ability of respiratory-deficient strains to mount an inducible adaptive response upon exposure to H_2O_2, it has been suggested that oxidant sensitivity in these respiratory-deficient strains is due to some energy-requiring process that is needed for the detoxification of ROS or repair of oxidatively damaged molecules (49).

8. Other primary antioxidants

CCP has already been discussed (Section 1.1), while the other antioxidants listed in Table 1.1, polyamines, metallothionein and thioredoxin, are not directly related to the research presented in this thesis, and will therefore not be reviewed. Their functions are, however, still displayed in Table 1.1.

1.5 Signal Transduction in Yeast

Recent work has shown that yeast cells possess similar signal transduction pathways to mammalian cells (22). A major difference appears to be that these signaling pathways are used for other purposes, i.e. the primary signal and the final target(s) are different.

The main glucose repression pathway

Glucose is undoubtedly one of the most prominent primary messengers in yeast cells and causes the activation or inactivation of many proteins, as well as the induction or repression of many genes. The addition of glucose to stationary-phase yeast cells triggers a wide variety of regulatory phenomena, and usually results in changes that favor fermentation and repress respiration (22). Two signaling pathways in yeast, the main

glucose repression pathway and the *ras*-adenylate cyclase pathway, are both induced by glucose (Figure 1.4)

The main glucose repression pathway's primary function is to switch off respiration during growth on high levels of glucose, or other rapidly fermentable carbon sources, by repression of genes involved in the Krebs cycle and ETC. The most important gene required for the repression exerted by the pathway is *HXK2*, which encodes hexokinase PII. Mutations in this gene affect glucose repression and stop the downstream activation of *CAT1 SNF1*, a protein kinase complex that inactivates a transcriptional repression complex (*MIG1-Ssn6 Cyc8-Tup1*), allowing the *MIG1*-encoded transcription factor to bind upstream regulatory sequences in the promoter of many glucose repressible genes (22). How hexokinase PII mediates its effects is unclear, as is the actual glucose sensing mechanism.

The ras-adenylate cyclase pathway

The addition of glucose to cells also results in activation of the *ras*-adenylate cyclase pathway by triggering a rapid transient increase in cAMP levels. Previous experiments have shown that intracellular acidification, and rapidly fermentable sugars such as glucose, mannose and fructose, are the primary triggers of the pathway. In the *ras*-adenylate cyclase pathway, the *RAS1* and *RAS2* gene products act on yeast adenylate cyclase, like the functional equivalents of the mammalian G_s proteins, activating adenylate cyclase to produce cAMP. cAMP then goes on to bind cAMP-dependent protein kinase (PKA), causing the dissociation of this enzyme's catalytic unit from its regulatory unit. The catalytic unit is then free to exert its effects on specific genes (see

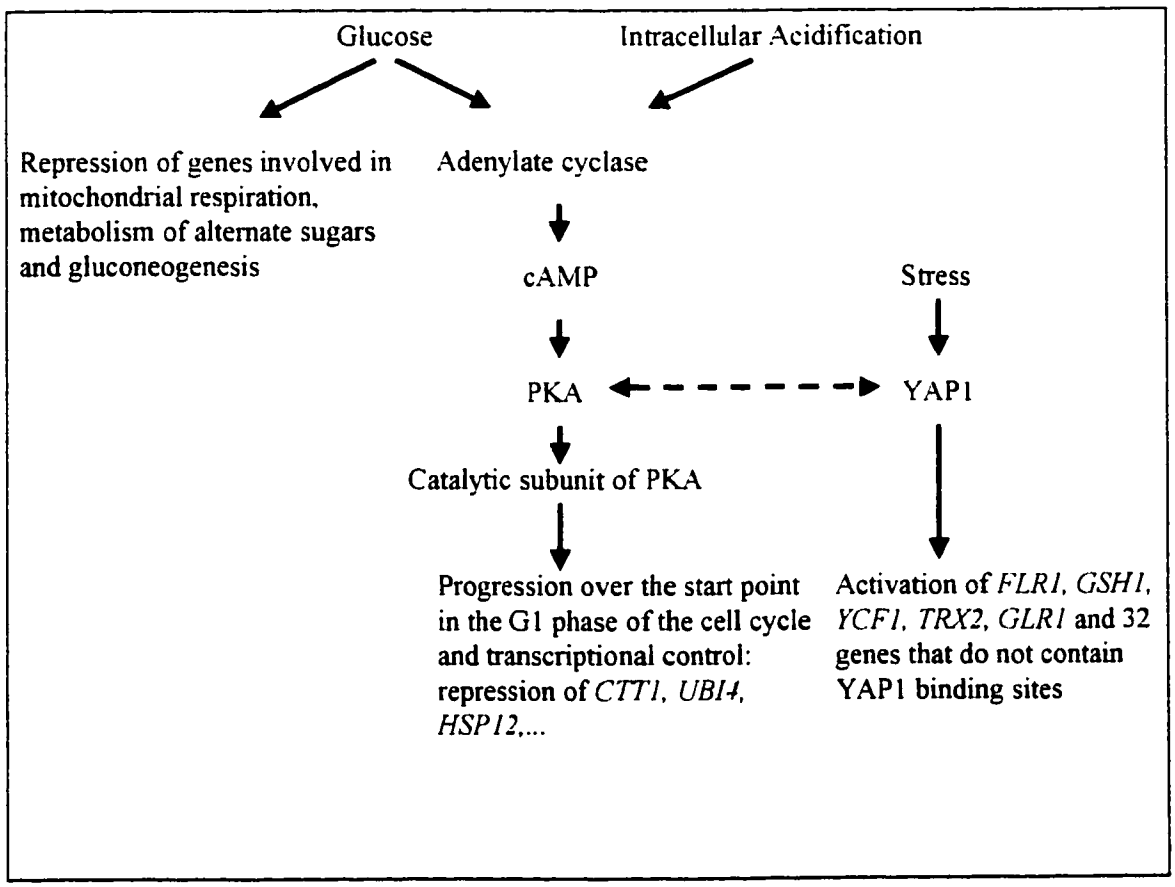

Figure 1.4 Signaling mechanisms involved in gene regulation and growth of yeast. Overview of the major targets and stimulating factors of the main glucose-repression pathway (extreme left), *ras*-adenylate-cyclase pathway (center) and the transcription factor Yap1p (extreme right). The broken arrow indicates that cross-talk can occur between both Yap1p, which has been shown to be required for activation of STRE genes, and PKA, which has been shown to inhibit transcriptional activation dependent on Yap1p. The "stress" signal activating Yap1p could be due to either nutritional or H_2O_2-induced stress. This figure is a modified version of Figures 1, 2 and 3 found in Reference 22.

below). This pathway has also been proposed to be involved in reproliferation from stationary phase (22).

Upon glucose starvation (at the diauxic shift) cAMP levels, which are characteristically high during exponential growth, dramatically decrease and remain at low levels during the post-diauxic and stationary phases (50). This leads to reduced levels of PKA, which appears to be a requirement for the activation of genes containing STRE elements. This is illustrated by experiments showing that mutations in the gene encoding the regulatory subunit of PKA, *BCY1* (which causes the constitutive activation of PKA) virtually eliminates STRE activation (23). Genes with known STRE elements include *UBI4* encoding ubiquitin, *HSP104* and the *HSP70*-related gene *SSA3* encoding heat-shock proteins, and *CTT1* encoding catalase. STRE elements are not only activated due to nutritional stress, but also due to oxidative stress, heat shock and ethanol stress (38).

Yeast strains with too little or too much activity of the *ras*-adenylate cyclase pathway display strongly pleiotrophic phenotypes, indicating that many potential targets for phosphorylation by PKA exist. An overactive pathway causes sensitivity to heat shock, nutrient starvation, failure to arrest properly in the G1 phase of the cell cycle upon nutrient limitation and inability to grow properly on nonfermentable carbon sources. Reduced activity of the pathway causes enhanced stress resistance and constitutive expression of genes normally only expressed in stationary phase. When activity of the *ras*-adenylate cyclase pathway is extremely low, the cells arrest in G_0 (22).

Yap1p

The *ras*-adenylate cyclase pathway is not the only factor involved in the increased resistance to H_2O_2 seen in stationary-phase yeast cells. Resistance to H_2O_2 is also mediated in part by the c-jun-related proteins, Yap1p and Yap2p (29). Yap1p and Yap2p are transcription factors, which are considered to belong to the family of AP1 factors (51-53). AP1 factors are found in eukaryotic organisms from yeasts to humans (54-56), and stimulate the expression of specific classes of genes in response to a wide variety of extracellular stimuli. In yeast, the Yap1p response element (YRE) contains a consensus 5'-TTAGTC/AA-3' sequence, which exists in promoters of *FLR1*, *GSH1*, *YCF1*, *TRX2* , and *GLR1* (29,57,58).

Loss of Yap1p function results in decreased resistance to H_2O_2 due to the reduced transcription of at least four genes involved in maintaining the redox status of the cell, *GSH1* (57), *TRX2* which encodes thioredoxin (59), *YCF1* which encodes an ATP-binding transporter (60) and *GLR1* (25). Moreover, recent evidence shows that Yap1p actually controls a large oxidative-stress response, and in response to H_2O_2, up regulates at least 32 proteins, 15 of which also require SKN7, another yeast transcriptional regulator (14). When challenged with H_2O_2, Δ*yap1* strains show greater susceptibility to H_2O_2-induced stress during stationary phase compared to their isogenic wild-type counterparts (29). They are, however, still able to adapt to H_2O_2-induced stress (29). This adaptation indicates that proteins other than the ones regulated by Yap1p are involved in response to oxidative stress. Steady-state levels of *GSH1* transcripts in exponential-phase, as well as levels under conditions of oxidative stress, are known to be reduced in Δ*yap1* mutants (29), as are total levels of glutathione during both stationary and exponential phase (26)

Yap1p has also been shown to be responsible for catalase induction in response to oxidative stress (14), and is known to be required for activity of the STRE element. Support for this comes from experiments performed using a *cdc25 yap1* double mutant. A *cdc25* mutation results in constitutively inactivated PKA by affecting the GTP exchange protein involved in activating *ras* in the *ras*-adenylate cyclase pathway. Therefore, enzymes usually repressed by PKA activity have high activity in these *cdc25* strains. However, this high activity is abolished in the *cdc25 yap1* double mutant, which shows only 12% the activity of the *cdc25* mutant when reporter genes, containing fused STRE-*lacZ* elements, are measured for β-galactosidase activity (61).

Furthermore, through the use of a *YAP1*-deficient yeast strain, Grant et al. have shown that the 3-fold increase in yeast *GLR1* expression during stationary phase is due entirely to Yap1p (26). They also demonstrate a stationary-phase increase in Yap1p transcriptional levels of less than 45% so that in order to explain the 3-fold increase in *GLR1* expression, some posttranscriptional regulation of Yap1p activity must exist. How Yap1p is regulated, transcriptional regulation or posttranscriptional regulation, upon both *S. cerevisiae's* entry into stationary phase and its exposure to oxidative stress, is not well understood.

A number of interesting similarities exist between the role of Yap1p in yeast and the role of AP1 in mammals. For example, both transcriptional complexes appear to play an integral role in the response of cells to certain kinds of environmental stress (59). Moreover, the activity of both transcription factors is rapidly induced following the addition of H_2O_2 to cells (62-64) in a mechanism that does not involve *de novo* protein synthesis (59). The c-jun component of the AP1 complex in mammals is known to be

regulated by phosphorylation events that modulate either its DNA binding domain or the transcriptional activity of the protein (65-68). As a number of potential phosphorylation sites exist in Yap1p (59), regulation of Yap1p by phosphorylation has been postulated by Kuge et al., but this form of regulation in *S. cerevisiae* has not yet been demonstrated. This is not the case in *S. pombe*, where the Yap1p ortholog, Pap1p, is constitutively cytoplasmic in strains carrying a mutation in the MAP kinase, Sty1p (69). This results in less transcription of PAP1p-controlled genes as PAP1p cannot enter the nucleus to transcribe them.

It is known that, upon exposure of oxidative stress, a small increase in the DNA-binding capacity of Yap1p occurs; however, the major change is at the level of nuclear localization. Upon induction, Yap1p relocates from the cytoplasm to the nucleus where it can induce transcription (70). Further evidence suggests that a cysteine-rich domain (CRD) at the C-terminus is critical for the function of this protein (69,70). The removal of one of three conserved cysteines in this domain results in the nuclear location of Yap1p due to the inability of it to bind a nuclear transporter, Crm1p (69). This suggests that oxidation of these cysteine residues may regulate Yap1p function.

Based on experiments that show decreased Yap1p transcription in Δ*bcy1* strains (strains lacking the regulatory subunit of PKA), it has been suggested that high levels of PKA (71) inhibit Yap1p dependent transcription. This inhibition is thought to occur through two mechanisms. Firstly, by diminishing YAP1 RNA and protein levels as demonstrated by their 2- to 3-fold reduction in Δ*bcy1* strains. Secondly, via an effect on occupancy of YRE's, which is based on the observation that high levels of PKA do not inhibit transcription by a Yap1p-LexA fusion protein at promoters dependent on LexA,

but do inhibit transcription at promoters dependent on Yap1p. It is not known why Yap1p cannot occupy these sites.

In conclusion, based on the observation that Yap1p is dependent on PKA activity (71), and that STRE activation is dependent on Yap1p (61), there seems to be an interaction between the *ras*-adenylate-cyclase pathway and the Yap1p transcription factor. This means that both signals are likely coordinately involved in the expression of genes under stress conditions in yeast cells. Although the main glucose-repression pathway and *ras*-adenylate-cyclase pathway are activated by glucose and seem to be involved in cell growth, both these pathways as well as Yap1p are able to contribute to the induction of antioxidant genes. An overview of all three pathways, and how cross-talk could occur between them, is shown in Figure 1.4.

1.6 H_2O_2-Induced Signaling

Although considered a toxic byproduct of respiration, there is recent evidence to suggests that H_2O_2 is necessary for certain signal transduction mechanisms in mammals. This is demonstrated by its involvement in processes such as bone resorption, cell growth, chemotaxis and apoptosis (31,32). Cellular regulation dependent on H_2O_2 makes up part of a bigger field of study that is expected to generate a flurry of research activity in the near future, "redox signaling" (32). Little, if any, experiments involving H_2O_2-mediated signaling in yeast have been performed, so all information concerning this topic pertains to mammalian cells.

Signal transduction proceeds via activation of second messengers such as cAMP, cGMP, inositol 1,4,5-triphosphate, transcription factors or nitric oxide by a primary signal. The second messengers formed then go on to influence cellular processes such as gene expression or cell proliferation. Other processes involved in second-messenger generation include specific receptors, adapter proteins, protein kinases and protein phosphatases.

H_2O_2 has been shown to mimic the stimulatory effects of insulin on glucose transport and lipid synthesis in adipocytes (31), activate transcription factors such as NF-kB and AP1 which influence gene expression (31,32), and stimulate Ca^{2+} release and protein phosphorylation (72). In particular, H_2O_2 results in oxidation of pyridine nucleotides causing Ca^{2+} release from mitochondria (72) and, in the nanomolar to micromolar concentration range, causes inhibition of protein tyrosine phosphatases (PTP's), which were recently shown to be dependent upon GSH concentration for their reactivation (43,73). Direct evidence that H_2O_2 plays a role in signaling cascades is shown by experiments involving platelet derived growth factor (PDGF) and the PDGF receptor. The stimulation of vascular smooth muscle cells (VSMCs) in rats by PDGF results in a transient increase in H_2O_2 that has been determined to be essential in order for the responses mediated by PDGF to take place. These responses, including tyrosine phosphorylation, MAP kinase activation, DNA synthesis, and chemotaxis are all inhibited when the PDGF-stimulated rise in H_2O_2 concentration is blocked (74)

In the field of H_2O_2-induced signaling, there are three important steps that require more research: (1) the mechanism by which H_2O_2 is generated in response to receptor stimulation in nonphagocytic cells, (2) the molecules on which H_2O_2 acts to propagate the

signal, and (3) the controlled pathway by which H_2O_2 is timely removed. Studies on these three processes, production, target, and elimination of H_2O_2, are expected to be an important area in biochemistry (31).

In phagocytic cells, $O_2^{\bullet -}$ (and through the action of SOD, H_2O_2) is produced via NADPH oxidase which is activated via protein-protein interactions involving SH3-proline-rich domains and phosphorylation by various protein kinases. In contrast, the mechanism of production of receptor-generated H_2O_2 production in nonphagocytic cells remains unclear (31).

Since H_2O_2 is a mild oxidant, it is thought that it can propagate its signal by acting on specific protein sulfhydryl groups, producing proteins with cysteine sulfenic acid (CysS-OH) or disulfide residues, both of which can easily be reduced back to Cys-SH by various cellular reductants. Very few proteins are expected to have a Cys-SH that is susceptible to oxidation by H_2O_2 as the Cys-SH would need a pK_a below 7.0 (31), whereas the pK_a values of most protein Cys-SH residues are higher than 8.0. A class of proteins that do contain Cys-SH residues with pK_a's low enough to be affected are PTP's. It is through these Cys-SH groups that H_2O_2-mediated inhibition of PTP's is believed to occur (73). Interestingly, several protein kinases such as PKA, cGMP-dependent protein kinase (PKG) and protein kinase C (PKC) all contain a Cys-SH residue within their active-site domain (31). It has been hypothesized, even though their pK_a values are not known, that oxidation of these conserved Cys residues is related to the observation that the activity of these kinases are altered in cells treated with H_2O_2.

Members of the peroxiredoxin family have been postulated to be involved in the removal of H_2O_2 involved in signaling. Peroxiredoxins (prx) are proteins that reduce

H_2O_2 with thioredoxin (Trx) as an immediate electron donor, or proteins that have sequence similarity to these proteins (31). Like many signal transduction proteins, prx exist in multiple isoforms in mammalian cells. Furthermore, mammalian prx members overexpressed in various cultured cells have been shown to inhibit the H_2O_2 activation of c-jun, NF-κB and apoptosis. These results, as well as the observations that prx proteins were discovered in connection with a variety of seemingly unrelated cellular processes such as proliferation, osteoregulation and response to oxidative stress, suggest that prx regulate intracellular H_2O_2 concentrations involved in signal transduction (31). A yeast enzyme that uses Trx as an electron donor to reduce hydrogen peroxide is thioredoxin peroxidase and is encoded by the gene *TSA1* (31).

1.7 Outline of Thesis

The following chapters examine the role that CCP plays (1) under normal growth conditions, (2) under oxidative stress and (3) in cellular signaling cascades. The results from these studies will demonstrate that CCP is involved in protecting mitochondrial integrity under normal growth conditions, and is needed for maximum resistance to H_2O_2-induced stress. The increased susceptibility of Δ*ccp1* cells under H_2O_2-induced stress will be shown to be due, in part, to lowered activities of catalase and GLR, as well as lower levels of glutathione, compared with isogenic wild-type cells. Results demonstrating the creation of a Δ*tsa1* strain of *S. cerevisiae*, for the purpose of examining the role of a cytosolic peroxidase in cell signaling, are also presented.

CHAPTER 2

EXPERIMENTAL PROCEDURES

2.0 Yeast Strains and Media

The yeast strain used in this study was W303-1B (*MATα*, *ade2*-1 *his3*-11,15 *leu2*-3,112 *ura3*-1 *trp1*-1 *can1*-100) which was kindly provided by Dr. Pam Hanic-Joyce (Concordia University). Isogenic wild-type cells were cultured in YPD medium (39) (2% glucose, 2% peptone (Becton Dickinson and Company) and 1% yeast extract (Becton Dickinson and Company). YPD media for Δ*ccp1* cells also contained 0.03% geneticin G418 (Gibco BRL). Cells were grown at 30°C with reciprocal shaking (300 rpm) in a Beckman incubator-shaker (39). Nonfermentative growth was carried out in 3% ethanol, 2% peptone and 1% yeast extract [YPE media (39)] or on YPG (39) plates which contained 3% glycerol (Fisher), 2% peptone, 1% yeast extract and 2% agar. YPDG (76) plates were prepared by adding 0.1% glucose to YPG plates. YPD plates were prepared by the addition of 2% agar to YPD media. Plates that were used for growth of Δ*ccp1* cells additionally contained 0.03% geneticin G418 (Gibco BRL). Exponential-phase cells were harvested at a culture optical density (OD_{600}) of 0.15. Stationary-phase cells were harvested after cultivation for 72 h (15). Cells grown on YPD, YPDG and YPG plates were incubated at 30°C for 2, 3 and 4 days respectively before cell counts were taken.

2.1 Disruption of the *CCP1* gene

Disruption of the CCP1 gene was carried out by Marcy Wright in our laboratory according to the following procedure (75). A 1632-bp PCR fragment was generated by using the pFA6-KAN4 plasmid (75), kindly donated by Dr. Howard Bussy, McGill

University, Montreal. This PCR fragment was generated using the *KAN* open reading frame (encoding for kanamycin resistance) as a template and primers 1 and 2, which contain sequences that flank the *CCP1* gene in the YKR066C ORF. Primer1 (5'ATTTCGCATTC ATGCAGACGCAAACACACACGTATATCTACAATTCAGCTGAAGCTTCGTACC-3'), the coding-strand PCR primer for the kanamycin gene (*KAN*), possesses 45 bases identical to the 5'-region of the yeast genome upstream of the *CCP1* start codon and 19 bases identical to the *KAN* sequence on its 3'-end. Primer 2 (5'-AATAATACGAAATAT AACCAATAAATAATATCTTTCC TCAGTGACTAGGCCACTAGTGGATCTG-3'), the antisense PCR primer for *KAN*, possesses 45 bases identical to the 3'-region of the yeast genome just after the TAG of *CCP1* and 19 bases identical to the *KAN* sequence on its 3'-end. PCR reactions (50 µl) contained Taq DNA polymerase buffer with $MgCl_2$ (Boehringer Mannheim), 1 µM primers (Biocorp Inc., Montreal), 200 µM dNTP's (Boehringer Mannheim), 5 units Taq polymerase (Boehringer Mannheim), 0.1 g of template DNA and DEPC-treated water. The template was amplified under the following conditions: 1 cycle of 5 min at 94°C to denature the template DNA; 26 cycles of 45 s at 94°C, 45 s at 55°C and 60 s at 72°C; 1 cycle of 10 min at 70°C. The PCR products were analyzed on a 1% agarose (Sigma) gel.

2.2 Transformation of Yeast

Yeast cells were transformed with 10-25 µl of PCR-generated DNA fragments using the lithium acetate method (76). Yeast cells were made competent for transformation

according to the following procedure: yeast cultures previously grown overnight were diluted to an OD_{600} of 0.4 in liquid YPD and grown until they reached an OD of 1.0. These cells (15 ml) were then pelleted at room temperature. Cells were then washed 1X in 15 ml of water and 2X in 15 ml of 100 mM Li Acetate (Arcos Organics), and resuspended in 150 µl of 100 mM LiAcetate. Cells (100 µl) were placed in 1.5-ml sterile tubes with 10 µl of carrier DNA (whale sperm DNA) that had previously been boiled for 10 min and cooled on ice. Transformation of these cells was carried out using the following procedure: 15 µl of the PCR product was placed in 1.5-ml sterile tubes containing 25 µl of the previously prepared carrier DNA/cell mixture, the tubes were incubated for 15 min at 30°C, 150 µl of LiAcetate PEG [800 µl 50% PEG-3350 solution (Sigma), 100 µl sterile water, 100 µl 1 M LiAcetate] was added and tubes were incubated for a further 40 min at 30°C. After this, 17 µl of DMSO (Fisher) was added and cells subjected to heat shock by placing the tubes in a 42°C water bath for 15 min. The cells were pelleted at room temperature, the LiAcetate PEG solution removed with a Pasteur pipette, and the cells were resuspended in 200 µl of YPD and incubated at 30°C for 4 h in a shaking incubator (200 rpm) before 100 µl was removed and plated onto YPD plates containing 0.03% geneticin. $G418^r$ transformants were selected after 48 h of growth on these plates

2.3 Verification of $G418^r$ Transformants by PCR

Correct targeting of the *KAN* gene to the genomic locus was verified by PCR using DNA extracted from transformed cells and primers 3-6. Primer 3 (5'-TTCTCCCGCAGC

TAGATCTC-3'), a coding-strand primer that binds 317 bases upstream of the start codon of the *CCP1* gene, was added to the same PCR reaction tube as primer 4 (5'- TCTGCAG CGAGGAGCCGTAAT-3'), an internal *KAN* primer located 172 bases upstream of the *KAN* start codon on the antisense-strand. Primer 5 (5'-TAAGGTTGTAGCAGTCGAGC-3'), an antisense primer 316 bases downstream of the *CCP1* stop codon, was added to a second PCR tube with primer 6 (5'-TGATTTTGATGACGAGCGTAAT-3'), an internal *KAN* coding-strand primer located at base 977 of the *KAN* gene. A PCR reaction was also run with primers 3 and 5. To obtain genomic DNA, about half a colony (~1 mm^3 of cells) was suspended in 100 µl of 10 mM Tris buffer (pH 8.0) containing 1% Triton X-100 (Sigma), 50 mM NaCl (ICN) and 1 mM EDTA (ICN). Acid-washed glass beads (0.1g) (Sigma) and 50 µl phenol/chloroform (1:1) were added and cells vortexed for 4 min. The cell lysate was centrifuged in an Eppendorf centrifuge at 14 000 rpm for 15 min at 4°C, 20 µl of the supernatant was transferred into a sterile tube and 5 µl of the aqueous phase was subjected to PCR. The PCR reaction conditions were the same as those used in the CCP disruption (Section 2.1), except that the 26 cycles following the template denaturation were run at: 45 s at 94°C, 45 s at 55°C and 2.5 min at 72°C. The PCR products were analyzed on a 1% agarose gel.

2.4 Disruption of the *TSA1* and *HO* genes

The methods used for the disruption, transformation and verification of the *TSA1* and *HO* genes are the same as those described above. The primers used in creating these disruptions (Biocorp Inc., Montreal), and experimental evidence for disruption are given

in Chapter 6. The PCR reactions were carried out on a PCR-PTC-100 Programmable Thermal Controller (MJ Research, Inc.)

2.5 Oxygen Consumption

Cellular oxygen uptake was measured at 30°C in a 1-ml stirred chamber using a Hansatech oxygen electrode following the manufacturer's instructions (21). Cells were grown for the desired time as described in Section 2.1 before aliquots were removed and diluted in fresh medium to 3 x 10^7 cells/ml and tested for oxygen consumption over the course of 5 min. Calibration of the electrode was accomplished using distilled water containing sodium dithionite (Fisher) ($[O_2] = 0$) and distilled water air-equilibrated to 20°C ($[O_2] = 260$ μM) (19). Cell counting was performed on all aliquots to determine the exact number of cells in the chamber. Cell counting was performed by diluting cells to a density of 1 x 10^6 cells/ml in 100 mM potassium phosphate (Kpi) buffer (pH 7.4) and counting at least 400 cells with a hemacytometer. Viability of the cells in the chamber was assessed by resuspending the cells to a density of 1 x 10^6 cells/ml in 100 mM Kpi buffer (pH 7.4) containing 0.01% methylene blue (Betz Laboratories) (77). After incubating at room temperature for 1 h, the percentage of dead cells (cells that took up the dye) was determined by counting both cells that did and did not take up the dye using a hemacytometer and bright-field microscopy. A minimum of 400 cells were counted. Cells boiled for 5 min were used as a control to make sure the assay was sensitive enough to detect dead cells.

2.6 Tests for Respiratory Competence

After growing cells for the desired amount of time in YPD medium at 30°C and 300 rpm in an incubator-shaker samples were diluted into both YPD or YPG media. The index of respiratory competence (IRC) was determined by plating 30 µl of each sample onto YPD or YPG plates to generate growth of around 300 colonies (21). The IRC was calculated from [(colonies on YPG) divided by (colonies on YPD)] x 100. The percent of $(rho)^+$ cells was determined by plating 30 µl of each sample, grown as described above and diluted to 3 x 10^4 cells/ml in 100 mM Kpi buffer (pH 7.4), onto YPDG plates. The percent of $(rho)^+$ cells is calculated from [(number of small colonies) ÷ (number of large colonies)] x 100. Plates used for Δ*ccp1* cells contained 0.03% geneticin.

2.7 Enzyme Assays

Total protein extraction was essentially the same as the method used by Izawa et al. (15). Yeast cells were grown to the desired phase in YPD medium at 30°C in an incubator-shaker set at 300 rpm, washed once with NET-NP buffer [(150 mM NaCl, 5 mM EDTA, 50 mM Tris-HCl (Sigma) pH 7.4, 0.5% NP-40 (Boehringer Mannheim)], and resuspended in NET-NP buffer containing 1 mM PMSF (Boehringer Mannheim) to a concentration of 1 x 10^{10} cells/ml. An equal volume of glass beads (0.5 mm) was added and the cells were disrupted by vigorous vortexing in 1.5-ml Eppendorf tubes for five 30-s intervals. Tubes were placed on ice for 30 s between vortexing. Cellular debris was removed by centrifugation at 15, 000 rpm for 1 min in an Eppendorf centrifuge.

Catalase activity was measured spectrophotometrically by monitoring the disappearance of H_2O_2 at 240 nm (ε_{240} = 4.36 x 10^4 cm^2/mol) in a final reaction volume of 1ml containing 33.3 μmoles Kpi buffer (pH 7.0), 13.33 μmoles H_2O_2 (Caledon) and 1-2 μg of protein from crude extracts (78). One unit of catalase activity catalyzes the disproportionation of 1.0 μmol of H_2O_2/min at 22°C.

CCP activity was assayed by the method of Yonetani (5). Assay mixtures (1ml) contained 100 mM Kpi buffer (pH 7.0), 10 mM EDTA, 18 mM H_2O_2, x-y μM ferrocytochrome *c* and 0.5 mg protein from crude extracts. One unit of CCP activity is defined as the amount catalyzing the oxidation by H_2O_2 of 1.0 μmol of ferrocytochrome *c*/min at 22°C (ε_{550} = 27.6 mM^{-1} cm^{-1}).

GLR (GLR) was assayed by the method of Di Ilio et al.(79). Assay mixtures (1ml) contained 0.1 M Kpi buffer (pH 7.4), 1mM GSSG (Sigma), 0.1 mM NADPH (Boehringer Mannheim), 1 mM EDTA and about 0.5 mg of protein from crude extracts. One unit of GLR activity is defined as the amount that catalyzes the oxidation of 1.0 nmol of NADPH/min (ε_{340} = 6.3 x 10^3 M^{-1} cm^{-1}) by oxidized glutathione at 22°C. Total glutathione levels were determined using the DTNB-GSSG reductase recycling assay for GSH and GSSG described by Anderson (80) after protein removal with $HClO_4$ and the samples neutralized with KOH (81). The assay mixture (1ml) contained 0.1 M Kpi buffer (pH 7.0), 1 mM EDTA, 1.5 mg/ml DTNB (Boehringer Mannheim), 4 mg/ml NADPH, 6 units/ml GLR and 10 μl of crude extract. Total glutathione levels are reported in nmoles and based on the rate of formation of 5-thio-2-nitrobenzoic acid (TNB) (ε_{412} = 14150 M^{-1} cm^{-1}) from 5,5'-dithiobis(2-nitrobenzoic acid) (DTNB) at 22°C in the presence of NADPH and GLR. The rates were calibrated through the use of GSSG standards (80).

Phosphatase activity was assayed by monitoring hydrolysis of the universal phosphate substrate, p-nitrophenyl phosphate (Aldrich), at 405 nm (ε_{405} = 18 $mM^{-1}cm^{-1}$) in 0.1 M acetate, 0.05 M Bis-Tris and 0.05 M Tris at pH 7.0 (73). One unit of phosphatase activity catalyses the formation of 1.0 µmol p-nitrophenolate/min at 22°C.

PKA activity was determined in a 96-well filter plate according to the method of Pitt and Lee (90). The assay mixture (125 µl) contained 800 mM Tris-HCl solution (pH 7.4), 0.5 mM IBMX (Calbiochem), 10 mM DTT (Sigma), 10 mM $MgCl_2$, 0.1 mg/ml BSA (Sigma), 200 µM ATP (Boehringer Mannheim), 0.5 µCi ^{33}P-ATP (Boehringer Mannheim), µM substrate peptide and 50 µg of proteins from crude extracts. The Crude extract was added last and samples were allowed to incubate at room temperature for 5 min. The reaction was stopped by adding 100 µl of 100 mM H_3PO_4 and incubated for a further 5 min at room temperature before being filtered under vacuum. The residue was washed 4-5 times with 150 µl 100 mM H_3PO_4 and radiation counts determined with a Microbeta (Wallac). PKA activity was determined by measuring the phosphorylation of the PKA peptide substrate (GRTGRRASL) (California Peptide Research Inc) with ^{33}P-ATP in the presence of the PKA inhibitor (TYADFIASGRTGRRNAI) (California Peptide Research Inc) and subtracting this value from the activity determined by phosphorylation of the PKA peptide in the absence of the inhibitor.

cAMP activity was determined using the cAMP SPA direct screening assay system (Amersham Pharmacia Biotech [code RPA 559]) according to directions from the supplier. Proteins from crude extracts (50 µg) were placed into separate wells in a 96-well filter plate which each contained: cAMP tracer (^{125}I), cAMP specific antibody and SPA anti-rabbit reagent. The plate was sealed and incubated at room temperature for 15-

20 h and the amount of [^{125}I]cAMP bound to the fluomicrospheres determined by counting in a microtitre plate β scintillation counter for 2 minutes. cAMP activity was determined through the use of cAMP containing standards and is reported in pmol/mg protein.

Protein levels were determined by the method of Bradford (82) using reagents purchased from Bio-Rad. All spectroscopic assays were preformed in a Beckman Du 650 spectrophotometer.

2.8 H_2O_2 Challenges

H_2O_2 stock (Caledon 30% w/v) was used to prepare H_2O_2 solutions spectrophotometrically ($\varepsilon_{240} = 4.36 \times 10^{4}\ M^{-1}\ cm^{-1}$). The yeast cells were treated in essentially the same manner as described by Flattery-O'Brien et al. (83). Cells were grown in YPD in an incubator-shaker at 30°C and 300 rpm. Exponential-phase cells were harvested at an OD_{600} of 0.15 which corresponds to ~ 6×10^{6} cells/ml, and stationary-phase cells were harvested after 72 h by centrifugation at 4000 g for 5 min at 25°C. Cells were resuspended in 100 mM Kpi buffer (pH 7.4) and diluted with the same buffer to a density of 2×10^{6} cells/ml. Samples (5 ml) were exposed to various concentrations of H_2O_2 for a period of 1 h and cell survival was monitored by spreading (in duplicate) 30-µl aliquots of cells, diluted in the same buffer to a cell density of 3×10^{4} cells/ml on YPD plates to obtain viable cell counts after 48 h. For H_2O_2-adaptation experiments, exponential-phase cells harvested at an OD_{600} of 0.15 were resuspended in fresh YPD medium containing 0.5 mM H_2O_2 (or no H_2O_2, control), diluted to 2×10^{6} cells/ml and

grown at 30°C with shaking for 1 h. The cells were centrifuged, resuspended in 100 mM Kpi buffer (pH 7.4), and 5-ml samples were challenged to 10 mM H_2O_2 for 1 h. Cell survival was monitored as described above.

CHAPTER 3

THE ROLE OF CCP UNDER NORMAL GROWTH CONDITIONS

Introduction

An important first step in determining whether or not CCP exerts an important function in yeast cells is to examine the growth rate (or fitness) and viability of cells in which CCP is absent. The following experiments compare the growth of Δ*ccp1* cells to that of isogenic wild-type cells in both fermentable and non-fermentable medium. In addition, experiments determining viability and mitochondrial function with respect to time are also examined. These experiments show the lag phase to be shorter, and the maximum cell density lower, in Δ*ccp1* cells compared to isogenic wild-type cells. They also show that mitochondria in Δ*ccp1* cells undergo time-dependent inactivation, despite a cellular survival rate of close to 100%.

Results and Discussion

Growth of Δccp1 Strain in Batch Culture

To determine if CCP is important under normal growth conditions, Δ*ccp1* and isogenic wild-type strains were grown on both fermentable (Figure 3.1) and nonfermentable (Figure 3.2) carbon sources. Growth curves were initiated by inoculating 50 ml of fresh medium, with cells previously grown overnight to stationary-phase, to give an OD_{600} of 0.05. Δ*ccp1* and isogenic wild-type cells display almost identical growth on glucose except for two small differences: time spent in lag phase and maximum cell densities reached. The Δ*ccp1* strain spends 2.5 h in lag phase, compared to 4 h for the isogenic wild-type, and reaches a maximum cell density that is 10% lower (Figure 3.1). The fact that Δ*ccp1* cells re-enter the growth cycle quicker than isogenic wild-type

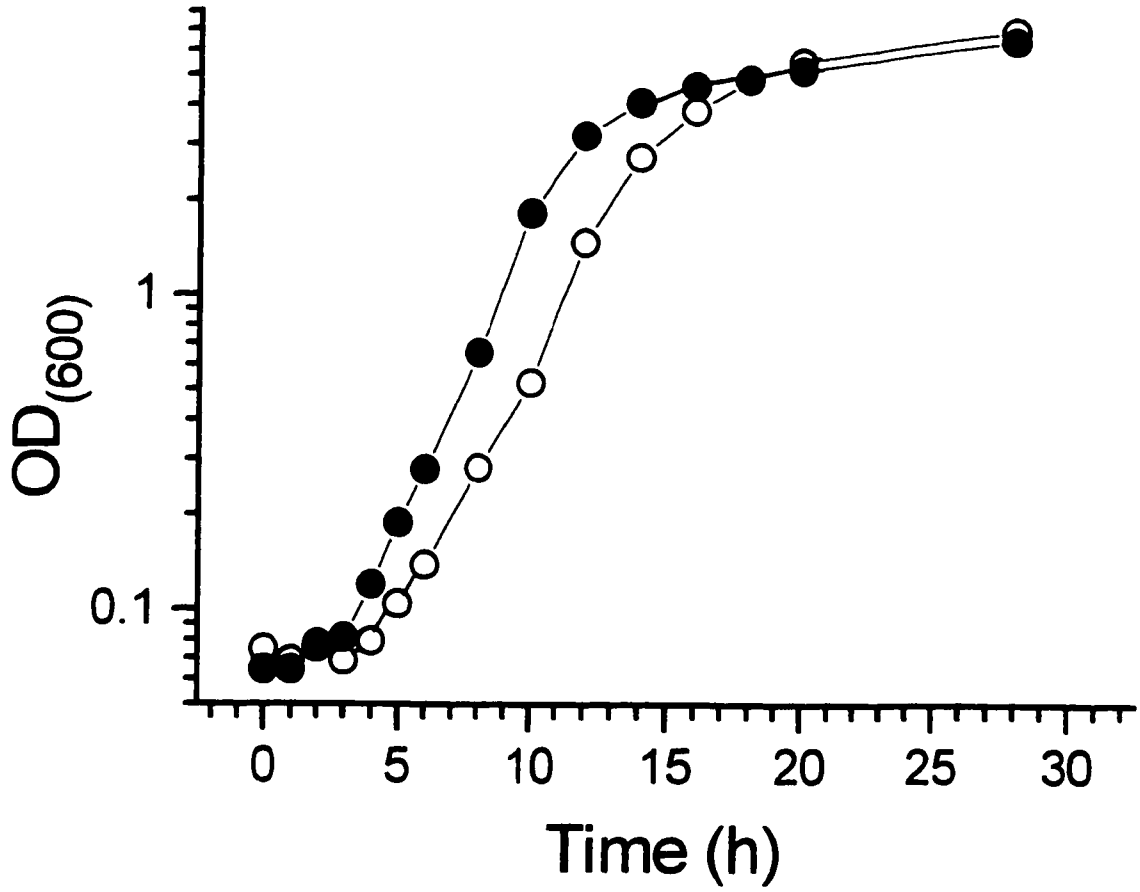

Figure 3.1 Comparison of growth of *Δccp1* (●) and isogenic wild-type (○) *S. cerevisiae* in fermentable medium. Cells were cultured in YPD medium at 30°C and growth was monitored by measuring the absorbance at 600 nm (OD_{600}). Data points are the average of three experiments and include experimental error. The experimental procedures are given in Section 2.0.

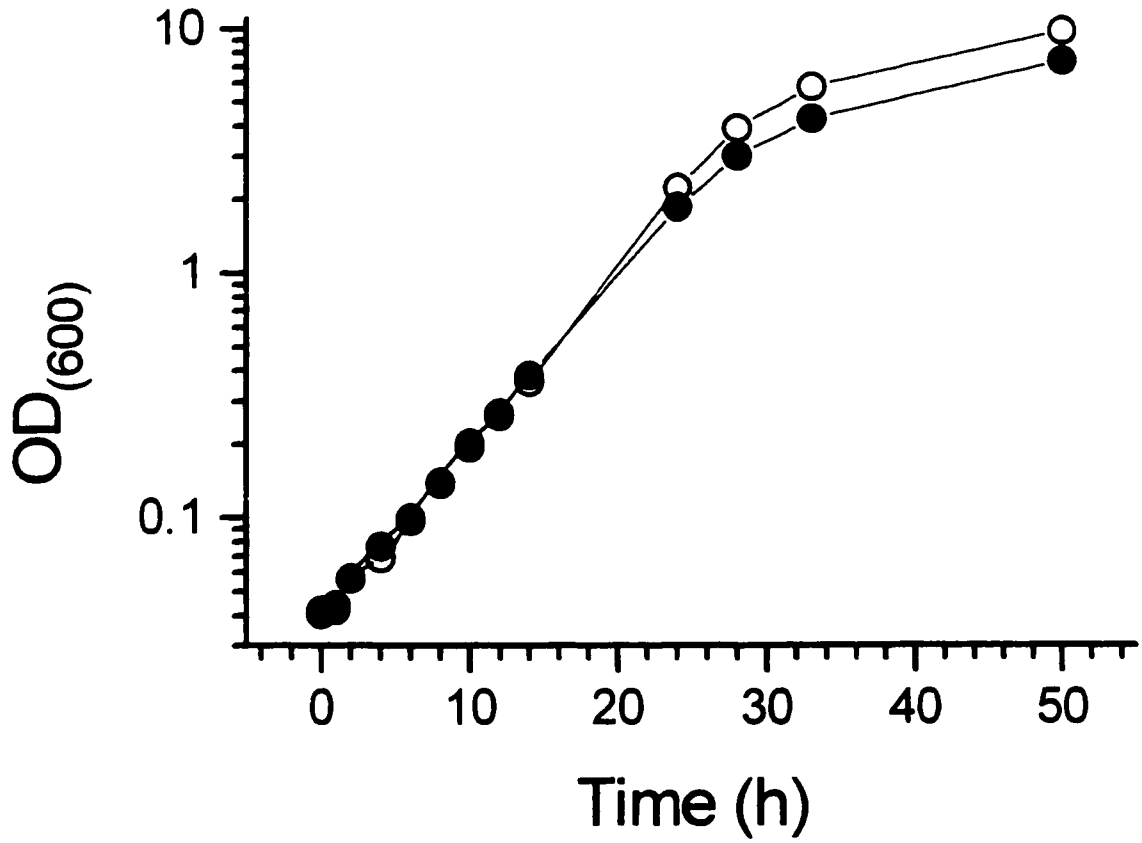

Figure 3.2 Comparison of growth of Δ*ccp1* (●) and isogenic wild-type (○) *S. cerevisiae* in nonfermentable medium. Cells were cultured in YPE medium at 30°C and growth was monitored by measuring the absorbance at 600 nm (OD_{600}). Data points are the average of three experiments and include experimental error. The experimental procedures are given in Section 2.0.

cells suggests that changes required for fermentative growth are already present, or are accomplished quicker, in Δ*ccp1* cells. If enzymes required for fermentative growth are already up regulated in Δ*ccp1* cells, it could mean that Δ*ccp1* cells present in overnight cultures only partially, or never, entered respiratory growth. As the main glucose repression pathway, as well as the *ras*-adenylate-cyclase pathway, are involved in reproliferation from stationary phase (22), it is possible that the quicker re-entry of Δ*ccp1* cells into the growth cycle is due to alterations in one or both of these pathways. It has recently been shown that lag times of *S. cerevisiae* containing disruptions in *MIG1*, which encodes a key transcriptional activator in the glucose repression pathway, are decreased by 50% (84).

Ca^{2+} levels may also be involved in the decreased lag time seen for Δ*ccp1* cells grown on glucose. Elevated Ca^{2+} levels have been shown to shorten the lag time in *S. cerevisiae* (85) and Ca^{2+} is known to be released by mitochondria, through oxidation of mitochondrial pyridine nucleotides, when elevated levels of mitochondrial H_2O_2 are present (86). As CCP has been shown to eliminate 53-55% of H_2O_2 generated at the level of the mitochondrial ETC, a major source of H_2O_2, and the cells used for inoculation in Figure 3.1 were undergoing respiratory growth elevated H_2O_2 is a possibility.

Growth of Δ*ccp1* cells on the nonfermentable carbon source, ethanol (Figure 3.2), suggests that Δ*ccp1* cells are capable of respiratory growth. Furthermore, there is no difference in the time taken to start respiratory growth. This suggests that proteins required for respiration were in fact up regulated in Δ*ccp1* cells grown overnight. However, like growth on glucose, the maximum cell density of Δ*ccp1* cells grown on ethanol is lower than that of isogenic wild-type cells, and the difference more pronounced

in ethanol (25% vs 10% lower). Because the growth rate is initially the same in isogenic wild-type and Δ*ccp1* cells, the data in Figure 3.2 suggest that Δ*ccp1* cells start out with fully competent respiratory function, but that this diminishes with time.

Mitochondrial Function and Integrity

Since the great majority of oxygen consumption occurs in mitochondria, it is considered a good test of mitochondrial function (21). The mitochondrial function of both Δ*ccp1* and isogenic wild-type cells was therefore evaluated by measuring the oxygen consumption of both strains over the course of seven days. Aliquots of cells from 50 ml cultures, growing at 30°C and 300 rpm, were removed and diluted to a cell density of 3 x 10^7 cells/ml. The cells were placed in a closed chamber, also equilibrated to 30°C, and their oxygen consumption monitored over the course of 5 min with rapid stirring.

Δ*ccp1* cells show slightly lower oxygen consumption, compared to isogenic wild-type cells, during their first three days of growth, exhibiting a 15% reduction (Figure 3.3). However, on their fifth and seventh days of growth, Δ*ccp1* cells exhibit a dramatic decrease in respiration, exhibiting only 35% the oxygen consumption displayed by isogenic wild-type cells. This decreased respiratory rate could explain the lower cell density reached by Δ*ccp1* cells when grown on glucose and ethanol (Figures 3.1 and 3.2). It should be noted that respiratory rates decline over the first few days of growth as a natural part of the establishment of stationary phase (44).

To determine whether or not the decreased respiration displayed by Δ*ccp1* cells was due to cell death, aliquots of cells were removed and percent viability determined (Figure 3.4) using the vital stain methylene blue as described in the experimental procedures

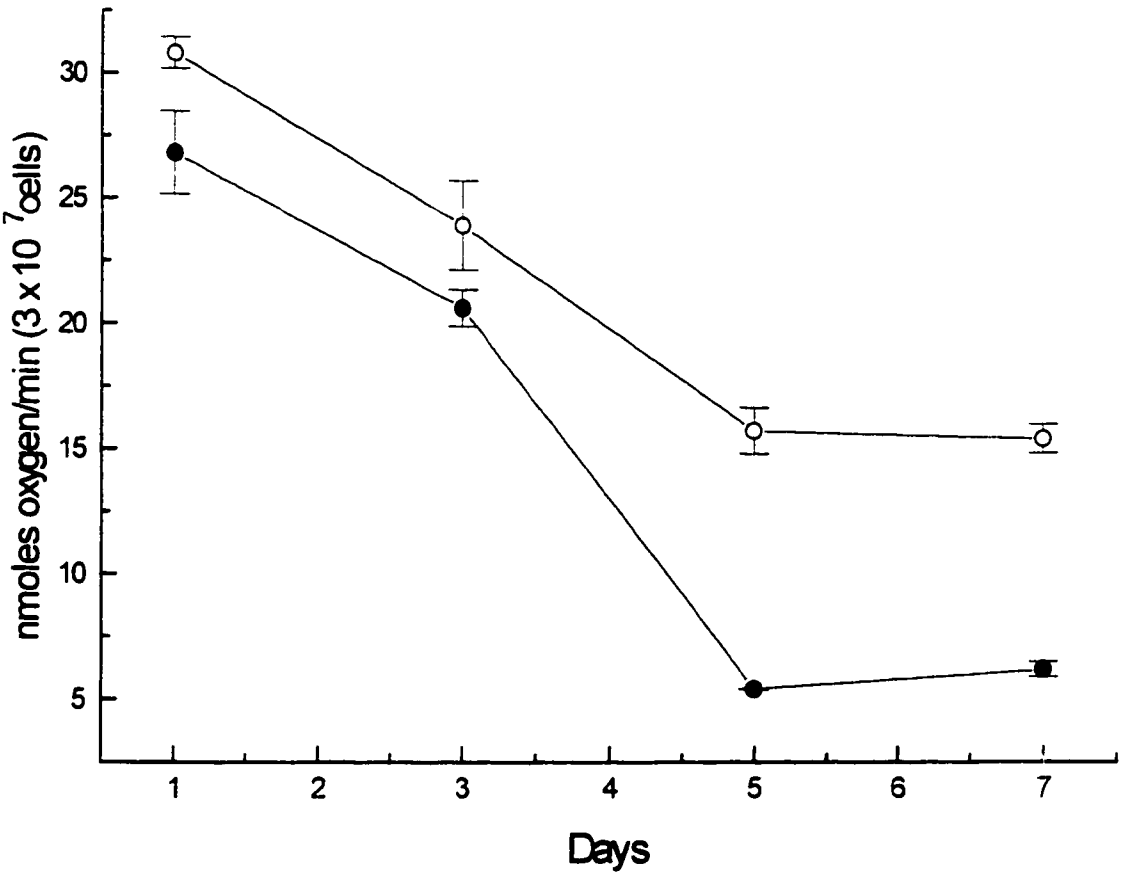

Figure 3.3 Comparison of oxygen consumption in Δ*ccp1* (●) and isogenic wild-type (○) *S. cerevisiae*. Cells were grown in YPD medium for the indicated times, diluted in fresh medium to 3 x 10^7 cells/ml and their oxygen consumption measured with a Hansatech oxygen electrode as described in the experimental procedures (Section 2.5). Data points are the average of three experiments.

(Section 2.5). To be sure this method was sensitive enough, the percent viability of yeast cells boiled for 5 min was used as a positive control. The percent viability of both strains over the course of 7 days was 97 to 99%, revealing that cell death was not the cause of the decreased respiration observed in *Δccp1* cells. The percent viability of heat-killed cells was always 0%.

In the absence of cell death, the most likely cause of decreased respiration is mitochondrial malfunction. Two tests were carried out to determine the extent of mitochondrial damage with time in *Δccp1* vs isogenic wild-type cells. In the first test, an index of respiratory competence (IRC) was determined (21) by plating equal aliquots of cells from each strain onto YPG and YPD plates. The number of colonies formed on YPG plates was divided by the number of colonies formed on YPD plates and multiplied by 100 to get % IRC. As YPG plates contain glycerol, any cells that contain non functional mitochondria are unable to grow; this test therefore enables one to determine the percentage of cells that have completely lost their ability to respire. The IRC values for both strains were determined over the course of 7 days and demonstrate that, whereas the isogenic wild-type cells maintain an IRC close to 100%, *Δccp1* cells gradually lose respiratory competence with time (Figure 3.5). On day 7, the *Δccp1* strain has an IRC of only 63.7% compared to 98% for the isogenic wild-type. The second test for mitochondrial competence involved plating single aliquots of cells onto YPDG plates, containing 3% glycerol and 0.1% glucose. Due to the presence of glucose, cells without functioning mitochondria ($[rho]^-$ cells) are still able to grow through fermentation. However, as there is only a low amount of glucose present, $[rho]^-$ cells form small colonies compared to cells with functioning mitochondria ($[rho]^+$) cells. Therefore, when

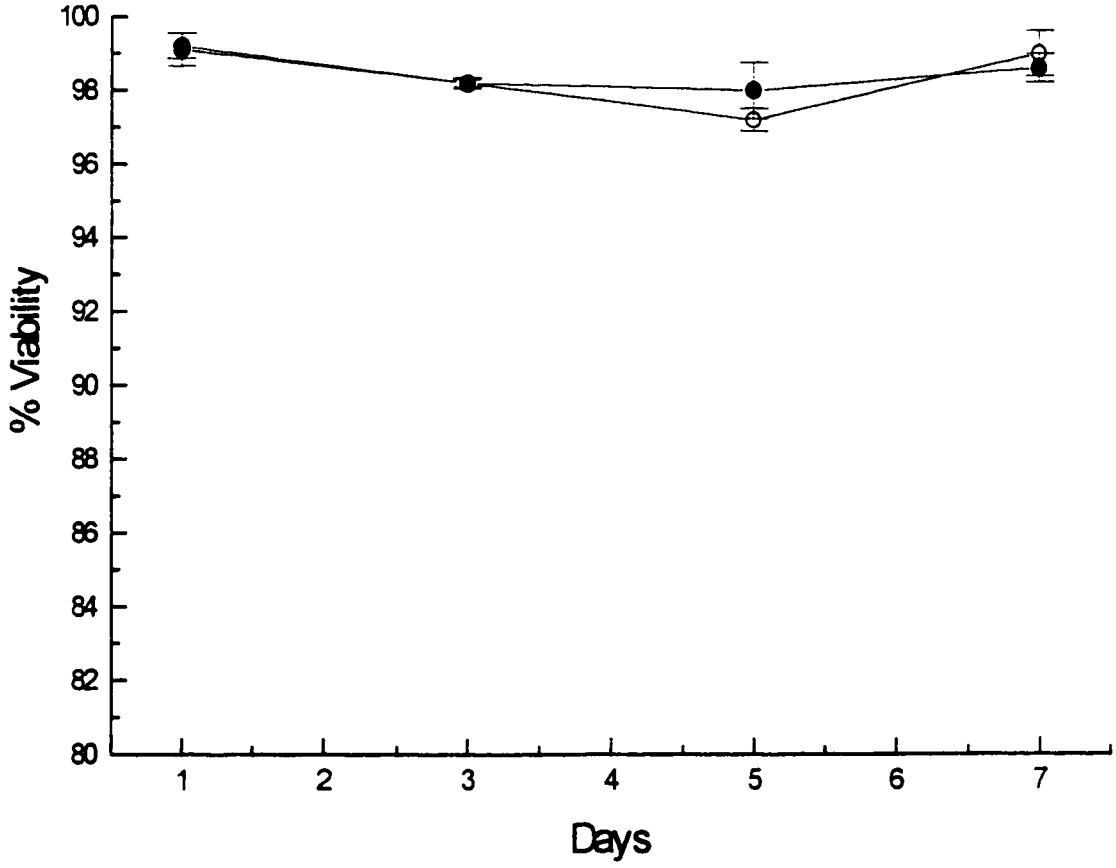

Figure 3.4 Comparison of percent viability in Δ*ccp1* (●) and isogenic wild-type (○) *S. cerevisiae*. Strains were grown in YPD medium for the indicated times, diluted to 1 x 10^6 cells/ml in 100 mM Kpi buffer (pH 7.4), and percent viabilities determined through incubation with the vital stain methylene blue as described under experimental procedures (Section 2.5). Data points are the average of three experiments.

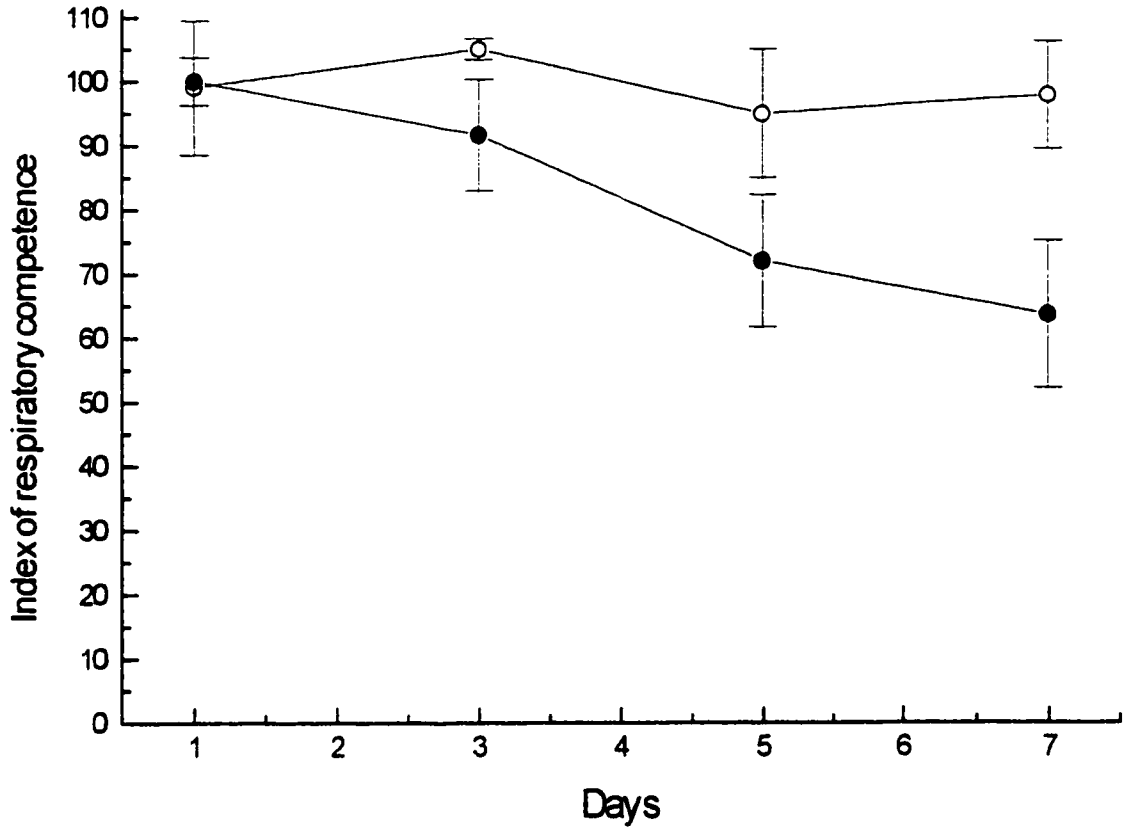

Figure 3.5 Comparison of index of respiratory competence (IRC) in Δ*ccp1* (●) and isogenic wild-type (○) *S. cerevisiae*. Strains were grown in YPD medium for the indicated times and their IRC determined as described under the experimental procedures given in Section 2.1. Data points are the average of three experiments.

an aliquot of cells is applied to YPDG plates, the percentage of cells that are [rho]$^-$ is determined by dividing the number of small colonies formed on the plate by the total number of colonies and multiplying this ratio by 100. The percentage of [rho]$^-$ cells in both strains, determined using YPDG plates, consistently remained between 97 and 98% over the course of seven days (Figure 3.6).

It is believed that mitochondrial components are very susceptible to oxidative stress (39). Perhaps the lack of CCP in Δ*ccp1* cells results in a buildup of H_2O_2 which by itself, or through formation of $OH^{\bullet}$ radicals (32), results in damaged mitochondria. It is apparent from both the IRC and oxygen consumption measurements that Δ*ccp1* cells appear to have close to normal mitochondrial function after the first day of growth, and relatively good mitochondrial function after 3 days of growth. This indicates that the cells used to inoculate the cultures involved in these assays were not respiratory incompetent. However, mitochondrial function in Δ*ccp1* cells is severely impaired on the fifth day of growth.

The oxygen consumption and IRC displayed by Δ*ccp1* cells also demonstrate the partial loss of respiration in the initially respiratory-competent Δ*ccp1* cells. The IRC of one-day old Δ*ccp1* cells is 100%, yet their oxygen consumption is 15% lower than that of the isogenic wild-type cells (Figures. 3.3 and 3.5). On day 7, the IRC in Δ*ccp1* cells is 63.7% compared to 100% for the isogenic wild-type cells, yet the oxygen consumption of Δ*ccp1* cells is ~ 33% that of isogenic wild-type cells. This partial loss in respiratory function could explain the decreased lag time and quicker entry of Δ*ccp1* cells into the fermentative mode of metabolism upon reproliferation from stationary phase.

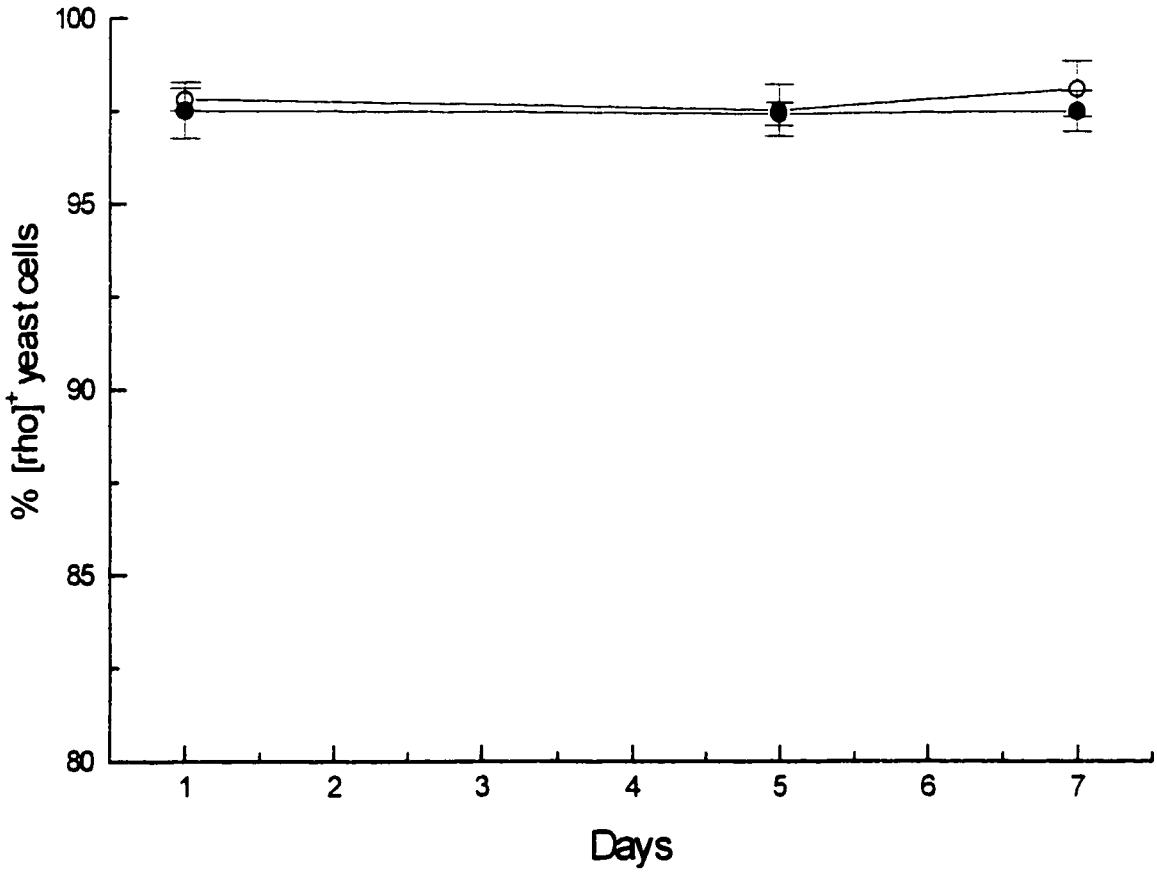

Figure 3.6 Comparison of percent $[rho]^+$ cells in Δ*ccp1* (●) and isogenic wild-type (○) *S. cerevisiae*. Strains were grown in YPD medium for the indicated times and the percent of $[rho]^+$ cells determined on YPDG plates as described under experimental procedures given in section 2.6. Data points are the average of three experiments.

The data in Figure 3.6 indicate that the damage to *Δccp1* mitochondria is enzymatic or structural, rather than permanent genetic damage. Cells with mitochondria that contain enzymatic or structural damage are able to repair this damage when grown on glucose where respiration is not essential, but are unable to produce enough energy to survive when required to grow directly on a nonfermentable carbon source (44). Since *Δccp1* cells display almost 100% relative growth on YPDG media (Figure 3.6), which contains a small amount of glucose, they are unlikely to be genetically damaged. However, the results obtained from the growth of *Δccp1* cells directly on YPG plates (Figure 3.5) suggests that there is some mitochondrial damage, which is likely structural or enzymatic.

Although genetic damage is probably not the primary reason for loss of mitochondrial function in these experiments, it does not necessarily mean that it is not occurring in *Δccp1* cells. H_2O_2 is known to induce DNA damage in yeast (38) and mtDNA is very susceptible to ROS induced stress (18). Hence, it would be surprising if *Δccp1* mtDNA was not subject to more H_2O_2-induced damage compared to isogenic wild-type mtDNA, especially in light of the significant damage to their mitochondrial proteins and/or membranes after 7 days. However, the frequency of mtDNA mutations is expected to be in the range of 10^{-4} to 10^{-6} per cell, which cannot be detected in the assays used above to examine mitochondrial function (21).

CHAPTER 4

THE ROLE OF CCP UNDER H_2O_2 –INDUCED STRESS

Introduction

It has previously been demonstrated that *S. cerevisiae* cells respond to H_2O_2-induced stress in exponential-phase cultures by increasing CCP activity (15) and expression of *CCP1* (45). This increased expression has been shown to be due to the transcriptional regulators Yap1p and Skn7p (45). Therefore, it appears that CCP may play an important role in protecting cells from H_2O_2-induced stress in exponential phase.

CCP activity (15), as well as *CCP1* transcription (24), have also been reported to increase in stationary-phase, compared to exponential-phase, *S. cerevisiae*. Stationary-phase yeast cells are considerably more resistant to heat and other stressors (28) due to the up regulation of a number of antioxidant enzymes and heat-shock proteins (23), as well as small antioxidants such as glutathione (41). Enzymes that are known to play major protective roles in stationary phase include GLR (26), and especially catalase (15). To determine how important CCP is in protecting cells from H_2O_2-induced stress in exponential and stationary phase, experiments were carried out determining the percent survival of both Δ*ccp1* and isogenic wild-type cells challenged to various concentrations of H_2O_2.

Another important factor in determining whether or not CCP is important for cell viability under H_2O_2-induced stress conditions is adaptation. It is well established that both eukaryotic and bacterial cells, when exposed to sublethal concentrations of certain stressors, are able to adapt and become tolerant to otherwise lethal concentrations. The term adaptation is used to describe this process when it occurs in *S. cerevisiae* (27,87). Izawa et al. have previously shown that catalase plays an important role in the adaptive

response (15), and more recently it has been shown that the synthesis of at least 115 proteins, including CCP, is stimulated by H_2O_2 (45). To test whether or not CCP plays an important role in the adaptation of *S. cerevisiae* to H_2O_2-induced stress, exponential-phase cells of both *Δccp1* and isogenic wild-type strains were pretreated with a sublethal concentration of H_2O_2 (0.5 mM) in fresh YPD for 1 h, following which they were challenged with a lethal concentration of H_2O_2 (10 mM) in phosphate buffer for 20-60 min.

Results and Discussion

Susceptibility of Exponential-phase Cells to H_2O_2-Induced Stress

To determine if CCP is important in protecting exponential-phase cells from H_2O_2-induced stress, cells were grown to an OD_{600} of 0.15 (early exponential phase) and challenged with various concentrations of H_2O_2 for a period of 1 h. Referring to Figure 4.1, it can be seen that *Δccp1* cells are more susceptible to H_2O_2-induced stress than the isogenic wild-type cells. This susceptibility appears to be negligible when challenged with low concentrations of H_2O_2, but, increases with increasing concentrations of H_2O_2 added, such that at 10 mM H_2O_2 the isogenic wild-type strain exhibits a 10-fold increase in percent survival. The high concentration of H_2O_2 required to effect a change in percent survival is likely due to the protective action of other H_2O_2-metabolizing enzymes. Cytosolic enzymes such as thioredoxin peroxidase and especially catalase, with its tremendously fast turnover rate, would presumably have to become saturated with H_2O_2 before the mitochondrial effects of the CCP deletion become apparent. It should be noted

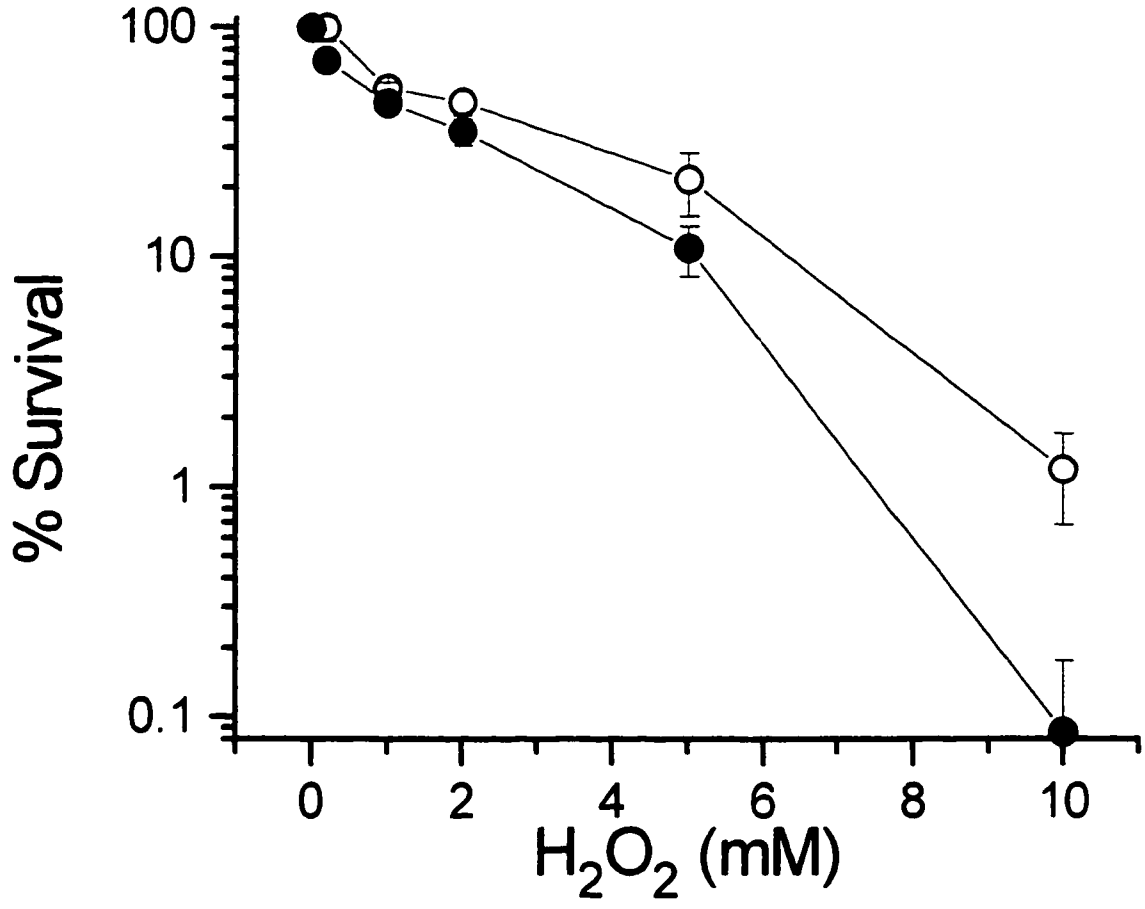

Figure 4.1 Susceptibility of exponential-phase Δ*ccp1* (●) and isogenic wild-type (○) *S. cerevisiae* to H_2O_2-induced stress. Cells grown to exponential phase in YPD were harvested and resuspended in 100 mM Kpi buffer (pH 7.4) to a density of 2 x 10^6 cell/ml and challenged for 1 h with 0.5, 1, 2, 5 and 10 mM H_2O_2. Viability was determined by diluting cells ~66-fold in fresh Kpi buffer and plating 30 µl onto plates containing YPD or YPD + geneticin for wild-type and Δ*ccp1* cells, respectively. Percentage survival is expressed relative to control cultures that were treated in a similar manner but not exposed to H_2O_2. Data points are the average of three independent experiments.

that, as metabolically generated H_2O_2 appears to damage *Δccp1* mitochondria over time (Chapter 3), exogenously added H_2O_2 also most likely results in increased mitochondrial damage in the *Δccp1* strain. However, as viability was quantified by growth on glucose, which permits the growth of respiratory-deficient cells, mitochondrial damage could not be assessed with this assay and would instead require growth on glycerol or other non-fermentable carbon sources for quantitation.

Susceptibility of Stationary-phase Cells to H_2O_2-Induced Stress

It was determined that CCP also plays a role in protecting *S. cerevisiae* from H_2O_2-induced stress during stationary phase (Figure 4.2). *Δccp1* cells display lower percent survival when challenged with 0-40 mM H_2O_2; for example, when challenged with 40 mM H_2O_2 for 1 h, exhibit 55% survival compared to 87% for the isogenic wild-type cells. These results indicate that CCP activity is important for the long-term survival of *S. cerevisiae*. The increased resistance to H_2O_2-induced stress demonstrated by stationary-phase *Δccp1* cells compared to exponential-phase *Δccp1* cells reveals that other protective mechanisms are also up regulated upon the transition to stationary phase.

As catalse has been shown to increase its activity 34-fold, and CCP 6-fold upon transition to stationary phase (15), it is surprising that CCP activity seems to play a role in protecting cytosolic components from H_2O_2-induced stress, especially when one considers that catalase is 10^3-fold more efficient at eliminating H_2O_2 in the mM range. Bearing in mind that percent viabilities compare growth on glucose (Figure 4.2), which is not inhibited by mitochondrial malfunction, the results of the stationary-phase H_2O_2 challenge suggest that cellular components other than mitochondria are being damaged

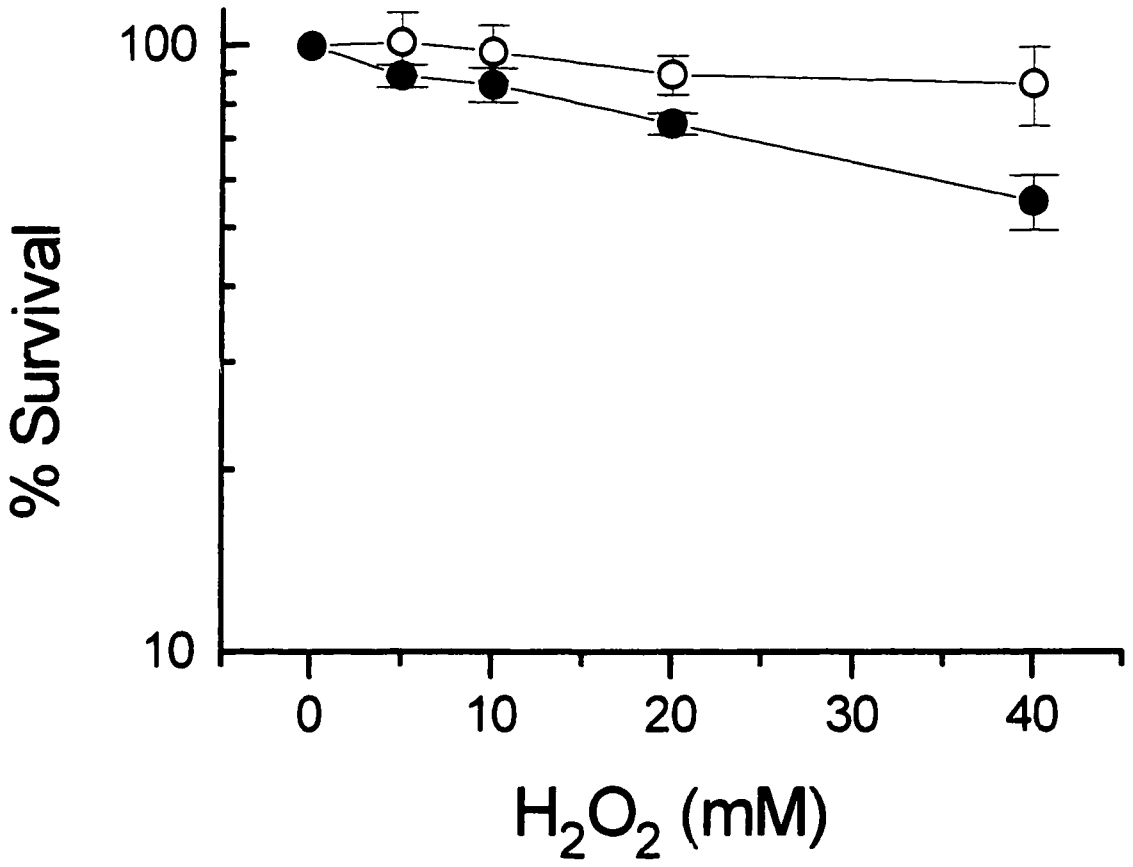

Figure 4.2 Susceptibility of stationary-phase Δ*ccp1* (●) and isogenic wild-type (○) *S. cerevisiae* to H_2O_2-induced stress. Cells grown to stationary phase (3 days growth) in YPD were harvested and resuspended in 100 mM Kpi buffer (pH 7.4) to a cell density of 2 x 10^6 cell/ml and challenged for 1 h with 5, 10, 20, and 40 mM H_2O_2. Viability was determined as in Figure 4.1. Percentage survival is expressed relative to control cultures that were treated in a similar manner but not exposed to H_2O_2. Data points are the average of three independent experiments.

from H_2O_2-induced stress.

Previous studies have revealed that mitochondrial function may play a role in protection against oxidative stress. It has been shown that [rho]$^-$ cells are more susceptible than [rho]$^+$ cells to H_2O_2-induced stress in exponential phase (49) and after 1 day of growth on YPD (27). Furthermore, it has been shown that treatment of yeast cells with respiratory inhibitors increase the sensitivity of these cells to H_2O_2 (25). Δ*ccp1* cells display a 15% lower respiratory rate, as well as a 10% lower IRC (Figures 3.3 and 3.5) compared to isogenic wild-type cells on their third day of growth (same day that stationary-phase tests for susceptibility to H_2O_2-induced stress were conducted). Therefore, as discussed in Section 1.4, respiratory rate might explain the increased sensitivity of Δ*ccp1* cells to H_2O_2-induced stress. However, the exposure of 5-day old Δ*ccp1* cells to 40 mM H_2O_2 for 1 h reveals that this is not likely (Figure 4.3). Since these cells have a 22% lower IRC compared to 3-day old Δ*ccp1* cells, yet the percent survival for both 3-day old and 5-day old cells, challenged to 40 mM H_2O_2 for 1 h, remains the same. This indicates that mitochondrial malfunction, in our experiments, does not explain the increased susceptibility of Δ*ccp1* cells to H_2O_2-induced stress. Five-day old isogenic wild-type cells show slightly increased susceptibility to H_2O_2-induced stress, and display the same IRC value, as their 3-day old counterparts.

Induction of Adaptation to H_2O_2-Induced Stress

Both Δ*ccp1* and isogenic wild-type cells are able to elicit an adaptive response (Figure 4.4) indicating that, despite its induction when *S. cerevisiae* is challenged to H_2O_2-induced stress (15), CCP is not crucial in the adaptive response and most likely

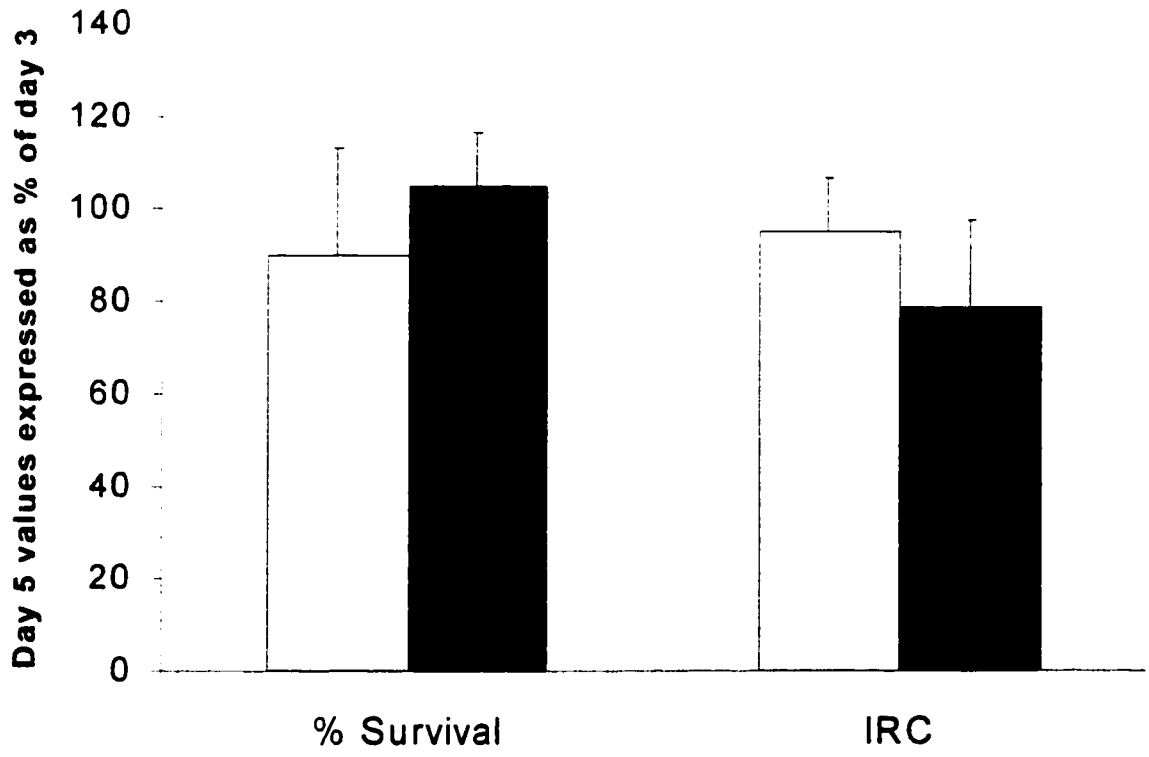

Figure 4.3 Values of IRC and percent survival on day 5 expressed as percentages of the day 3 values for Δ*ccp1* (dark bars) and isogenic wild-type (white bars) strains. The experimental procedures are given in Sections 2.5 and 2.6

plays a secondary role to other protective mechanisms that are also up regulated. The increased percent survival displayed by both pretreated and non-pretreated isogenic wild-type cells, compared to the corresponding *Δccp1* cells, can be explained by the increased tolerance of isogenic wild-type cells to exponential-phase H_2O_2-induced stress (Figure 4.1).

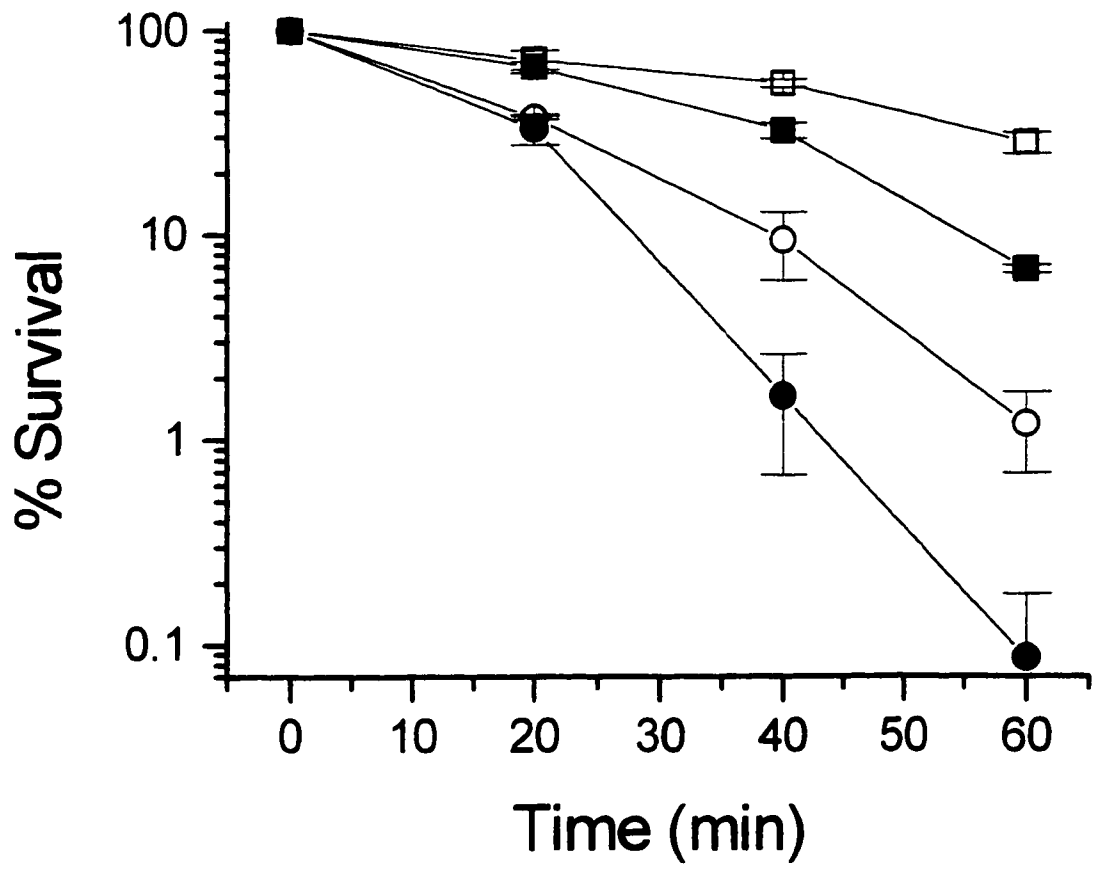

Figure 4.4 Effect of CCP deficiency on adaptation to 10 mM H_2O_2. Isogenic wild-type (O), pretreated isogenic wild-type (□), Δ*ccp1* (●) and pretreated Δ*ccp1* (■) cells were grown to exponential phase in YPD, harvested, and diluted to 2 x 10^6 cells/ml in fresh YPD containing no pretreatment (control) or pretreatment with a sublethal concentration of 0.5 mM H_2O_2. Samples were then grown for 1 h before being harvested and resuspended in 100 mM Kpi buffer (pH 7.4) to a cell density of 2 x 10^6 cell/ml. Samples were challenged with 10 mM H_2O_2 and cell survival monitored as described in Figure 4.1 over 60 min. Percentage survival is expressed relative to control cultures that were treated in a similar manner but not exposed to H_2O_2. Data points are the average of three independent experiments.

CHAPTER 5

A POSSIBLE ROLE FOR CCP IN CELL SIGNALING

Introduction

To determine if the increased susceptibility of Δ*ccp1* cells to H_2O_2 was, in fact, due to a loss of CCP activity, and not a decrease in other protective enzymes, the exponential and stationary-phase activities of CCP, catalase and GLR, as well as the levels of total glutathione (GSH and GSSG), were determined in both Δ*ccp1* and isogenic wild-type cells. The results of these experiments demonstrate a decrease in the stationary-phase activities of catalase and GLR and in the levels of glutathione, in both phases, for Δ*ccp1* cells. The concurrent down regulation of all species tested indicates that up regulation of the *ras*-adenylate cyclase pathway, or down regulation of Yap1p levels, might be occurring in Δ*ccp1* cells. This prompted further experiments, which led to the observation that key second messengers such as PKA and phosphatases are altered in Δ*ccp1* cells.

Results and Discussion

Changes in Enzyme Activities

Upon entry into stationary phase, all three antioxidant enzymes tested increase their activities (Table 5.1). In the isogenic wild-type strain, CCP increases its activity 3.5-fold, which is close to the previously reported value of 4.5 (15), catalase increases its activity 28-fold, compared to the previously reported 24-fold increase (15), and GLR increases its activity 3.2-fold, again close to the previously reported 4-fold increase (26). However, the induction of catalase and GLR is severely reduced in the Δ*ccp1* strain. Both isogenic

A. Exponential-phase Activity

Strain	Total Glutathione	CCP	Catalase	GLR
Wild-type	5.72 ± 0.60	2.06 ± 0.49	1.52 ± 0.20	18.8 ± 2.1
Δccp1	1.02 ± 0.20	N.D	1.27 ± 0.28	18.6 ± 1.3

B. Stationary-phase Activity

Strain	Total Glutathione	CCP	Catalase	GLR
Wild-type	7.92 ± 0.63	7.25 ± 0.20	42.3 ± 6.6	60.0 ± 1.3
Δccp1	2.16 ± 0.30	N.D	14.0 ± 3.4	29.2 ± 3.9

Table 5.1 Total glutathione levels, cytochrome *c* peroxidase (CCP), glutathione reductase (GLR) and catalase activities in isogenic wild-type and *Δccp1* yeast strains. Cells were harvested in exponential phase (**A**) or stationary phase (72-h growth) (**B**) and lysed with glass beads. Glutathione levels are reported as nmoles glutathione/10^9 cells. CCP activity is reported in m-units/mg protein where one unit of CCP activity is defined as the amount that oxidizes 1 μmol of ferrocytochrome *c*/min at 22°C. Catalase activity is reported in units/mg of protein where one unit of catalase activity is defined as the amount that catalyses the dismutation of 1 μmol of H_2O_2/min. Glutathione reductase (GLR) activity is reported in units/mg protein where one unit of (GLR) activity is defined as the amount that oxidizes 1 nmol of NADPH/min in the presence of oxidized glutathione. Values are means ± S.D of three experiments. N.D = not detected.

wild-type and Δ*ccp1* cells exhibit almost the same catalase and GLR activity in exponential phase, but. these activities increase only 11- and 1.6-fold respectively, upon entry of the Δ*ccp1* cells into stationary phase. This indicates that CCP activity may affect either one or both of these enzymes, or possibly the pathways that up regulate their activity upon entry into stationary-phase. Table 5.1 also shows glutathione levels to be greatly reduced in both stationary-phase and exponential-phase Δ*ccp1* cells. The Δ*ccp1* strain shows a 5.6-fold decrease in total glutathione during exponential-phase and a 3.4-fold decrease in stationary-phase.

The lower antioxidant enzyme activities in stationary phase, coupled with the decreased glutathione levels in both exponential- and stationary-phase Δ*ccp1* cells, suggest that the increased susceptibility of Δ*ccp1* cells to H_2O_2-induced stress may not simply be due to the absence of CCP-mediated H_2O_2 detoxification. Rather, the increased susceptibility seems to be due to a controlled down regulation of antioxidant defenses in stationary phase, and possibly decreased glutathione levels in both phases. The absence of *GSH1* has been shown to result in increased sensitivity to H_2O_2-induced stress during exponential phase, indicating that glutathione levels are important for protection during this growth phase (42). In addition, catalase and GLR are known to offer protection against H_2O_2 in stationary phase (15,26).

The simultaneous reduction in the enzyme activities in Table 5.1 and in glutathione levels can be explained by decreased Yap1p activity. Yap1p controls the transcription of glutathione and GLR through YRE's in the promoters of *GSH1* and *GLR1* respectively, and affects the transcription of STRE-controlled genes such as *CTT1* by acting downstream of PKA in the *ras*-adenylate cyclase pathway (22). Furthermore, a Δ*yap1*

yeast strain is identical to the Δ*ccp1* strain in that (i) it is sensitive to H_2O_2-induced stress (60), (ii) exhibits lower glutahione levels and (iii) lacks the normal stationary-phase increase in GLR activity (26). Moreover, results showing stationary-phase Δ*yap1* cells to be more resistant to H_2O_2-induced stress compared to exponential-phase Δ*yap1* cells (29) are also consistent with our results.

Since Yap1p is known to be necessary for the induction of a variety of proteins in response to H_2O_2-induced stress (14), it is curious that the Δ*ccp1* strain did not lose its ability to adapt (Figure 4.4) assuming that Yap1p levels are altered in Δ*ccp1* cells. However, previous experiments involving Δ*yap1* strains of *S. cerevisiae* demonstrate that like the Δ*ccp1* strain, these yeast cells are able to adapt to H_2O_2-induced stress (29). Although, in contrast to our results (Figure 4.4), Δ*yap1* yeast cells do not adapt to the same extent as their isogenic wild-type counterparts. This suggests that residual Yap1p activity still exists in the Δ*ccp1* yeast.

Decreased Yap1p activity could occur at the transcriptional or posttranscriptional level. Regulation of Yap1p by phosphorylation has been postulated by Kuge et al. as a number of potential phosphorylation sites exist in Yap1p (59). Moreover, Yap1p-dependent transcription is abolished in strains containing high levels of PKA (71), implicating control of Yap1p by the *ras*-adenylate cyclase pathway. An overactive *ras*-adenylate cyclase pathway (and therefore higher PKA activity) could also explain the decreased levels of catalase displayed by the Δ*ccp1* strain in stationary phase, and possibly the quicker entry of Δ*ccp1* yeast cells into the growth cycle (22) (Figure 3.1). It has also been suggested, due to the observation that stationary-phase GLR activity is severely reduced in petite strains of *S. Cerevisiae* (26), that Yap1p activation is under

mitochondrial control. Thus, perhaps the slightly impaired mitochondrial function displayed by Δ*ccp1* cells on their third day of growth (Figures 3.3 and 3.5) results in lowered Yap1p activity, which in turn results in lowered antioxidant enzymes and molecules. This cascade of events could explain the results of other researchers who showed that functioning mitochondria are necessary for maximal protection against H_2O_2-induced stress in both exponential phase (49) and stationary phase.

Change in PKA Activities

PKA assays, performed on exponential- and stationary-phase samples by Sylvie Desmarais at the Merck Frosst Centre for Therapeutic Research, are shown in Figure 5.1. Despite a relatively large error, PKA activity was determined to be higher in Δ*ccp1* cells in both exponential and stationary phase. The stationary-phase levels of active PKA in the Δ*ccp1* cells is about 1.2-fold higher compared to isogenic wild-type cells suggesting that factors other than PKA are also involved in the lower stationary-phase catalase activity displayed by Δ*ccp1* cells, which is about one third that of isogenic wild-type cells. The exponential-phase levels of active PKA are, however, much higher in the Δ*ccp1* strain when compared to the isogenic wild-type. In exponential-phase, Δ*ccp1* cells display 3-fold higher PKA activity compared to isogenic wild-type cells, which could account for the 16% decreased exponential-phase activity of catalase in the Δ*ccp1* cells compared to isogenic wild-type cells (Section 1.5).

Although the values reported in Figure 5.1 represent the average of 4 trials, they seem to display a fundamental error. Previous experiments on *S. cerevisiae* have shown PKA levels in stationary phase to be lower than PKA levels in exponential phase, the opposite

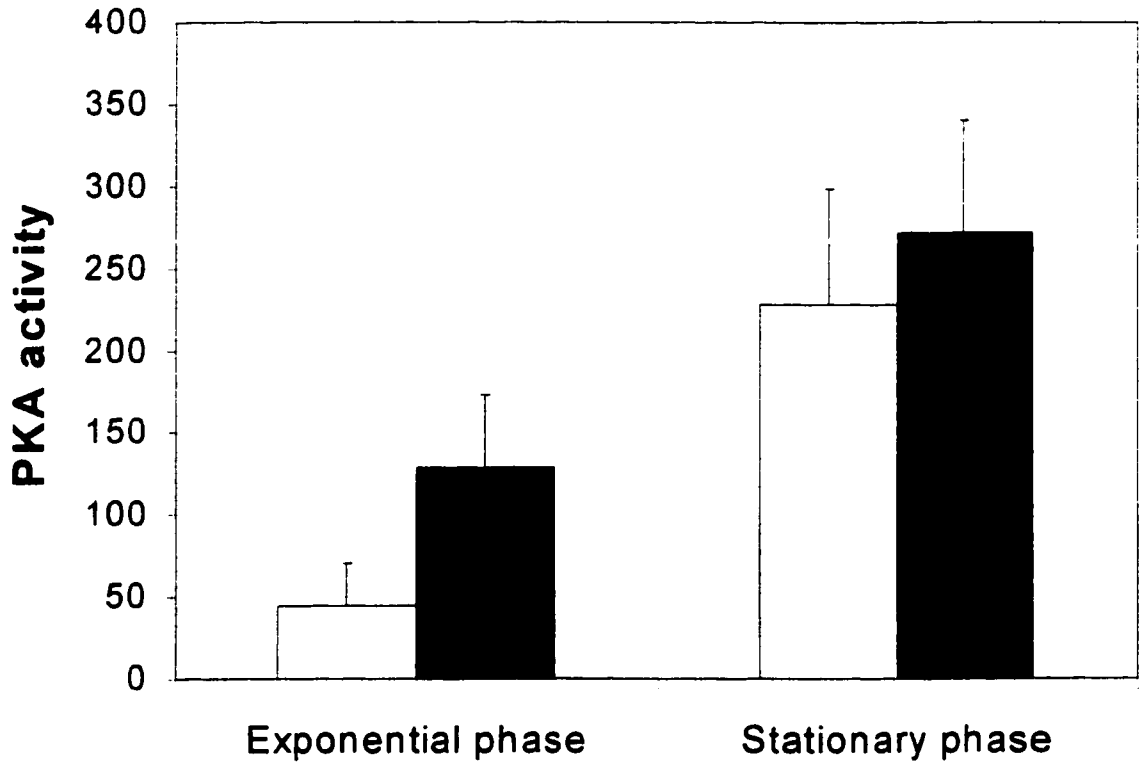

Figure 5.1 Comparison of exponential- and stationary-phase levels of PKA activity in Δ*ccp1* (dark bars) and isogenic wild-type cells (white bars). Cells were harvested in exponential or stationary phase and lysed with glass beads as discussed in Section 2.7. PKA activity is reported in units/50 μg protein where one unit of activity is defined as the transfer of 1 pmol of [γ-^{32}P]ATP per min at room temperature. Values are means ± S.D of three experiments.

of what is reported in Figure 5.1 (22,50). Interestingly, the 3-fold increase in PKA activity demonstrated by exponential-phase Δ*ccp1* cells, compared to exponential-phase isogenic wild-type cells, would explain the 3-fold decrease in catalase activity displayed by stationary-phase Δ*ccp1* cells. Perhaps exponential-phase cells were mixed up with stationary-phase cells. These experiments will have to be repeated before any reliable conclusions can be made.

Change in cAMP Levels

cAMP levels, performed on exponential- and stationary-phase samples by Dr. Douglas Pon at the Merck Frosst Centre for Therapeutic Research, are shown in Figure 5.2. cAMP acts directly upon PKA and causes release of its active subunit resulting in increased PKA activity. cAMP levels should decrease as cells enter stationary phase (22,50), however, wild-type cAMP levels, like PKA activity (Figure 5.1), increases upon entry of these cells into stationary phase (Figure 5.2). Because both cAMP levels and PKA activity were determined using the same tubes it seems likely that exponential and stationary phase tubes were in fact mixed up. The exponential- and stationary-phase levels of cAMP in Δ*ccp1* cells remains fixed at about 3 pmol/mg protein suggesting that cAMP levels are not properly regulated during growth. Due to the higher PKA activity displayed by Δ*ccp1* cells, it is surprising that these cells show lower cAMP levels compared to isogenic wild-type cells (Figures 5.2 and 5.3). Perhaps Δ*ccp1* cells attempt to deal with increased PKA activity by decreasing cAMP levels

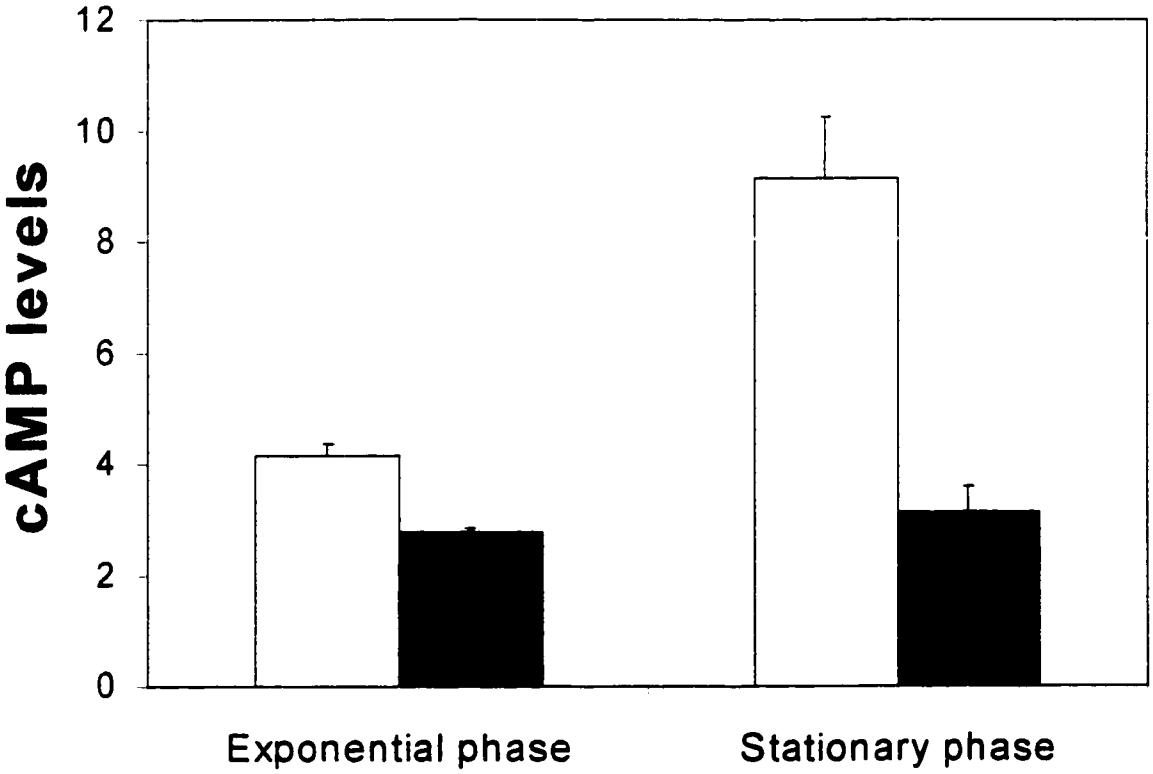

Figure 5.2 Comparison of exponential- and stationary-phase levels of cAMP in Δ*ccp1* (dark bars) and isogenic wild-type cells (white bars). Cells were harvested in exponential or stationary phase and lysed with glass beads as discussed in Section 2.7. cAMP levels are reported in pmol/mg protein. Values are means ± S.D of three experiments.

Change in Phosphatase Activities

Knowing that CCP is involved in removing physiologically generated H_2O_2, and that physiological increases in H_2O_2 influence signaling pathways through inhibition of protein tyrosine phosphatases (PTP's) (43,74), phosphatase activity was assayed in the Δ*ccp1* and isogenic wild-type strains. Total phosphatase activities were determined from crude extracts by monitoring the hydrolysis of the universal phosphate substrate, p-nitrophenyl phosphate (Figure 5.3). This assay reveals that total phosphatase activity in Δ*ccp1* cells is lower in both the exponential and stationary phases of growth, compared to total phosphatase activity in isogenic wild-type cells. Δ*ccp1* cells have 78.4% phosphatase activity in exponential phase and 69% in stationary phase relative to wild-type cells. Since this assay in not specific, it is not known if the lowered phosphatase activity is due to one specific class of phosphatases, such as PTP's, or if a variety of phosphatases are being inhibited.

CCP is responsible for the elimination of ~55% of mitochondrial H_2O_2 that would otherwise enter the cytosol (36). Perhaps the mitochondrial H_2O_2 released in the absence of CCP can inactivate phosphatases. At first thought one might assume that catalase, with its fast turnover of 10^7 sec^{-1} (13) may quickly get rid of extra cytosolic H_2O_2. However, due to the 10^3-fold increase in K_m displayed by catalase, when compared to CCP (Chapter 1), CCP with a K_m of ~10^{-5} can compete with catalase in the elimination of nM-μM H_2O_2, which are the levels needed for PTP inhibition (73). In the absence of CCP, small amounts of H_2O_2 should be able to leave the mitochondria, enter the cytosol, and inactivate phosphatases before catalase or cytosolic peroxidases could eliminate it. The absence of CCP could, therefore explain the decreased phosphatase levels seen in Δ*ccp1*

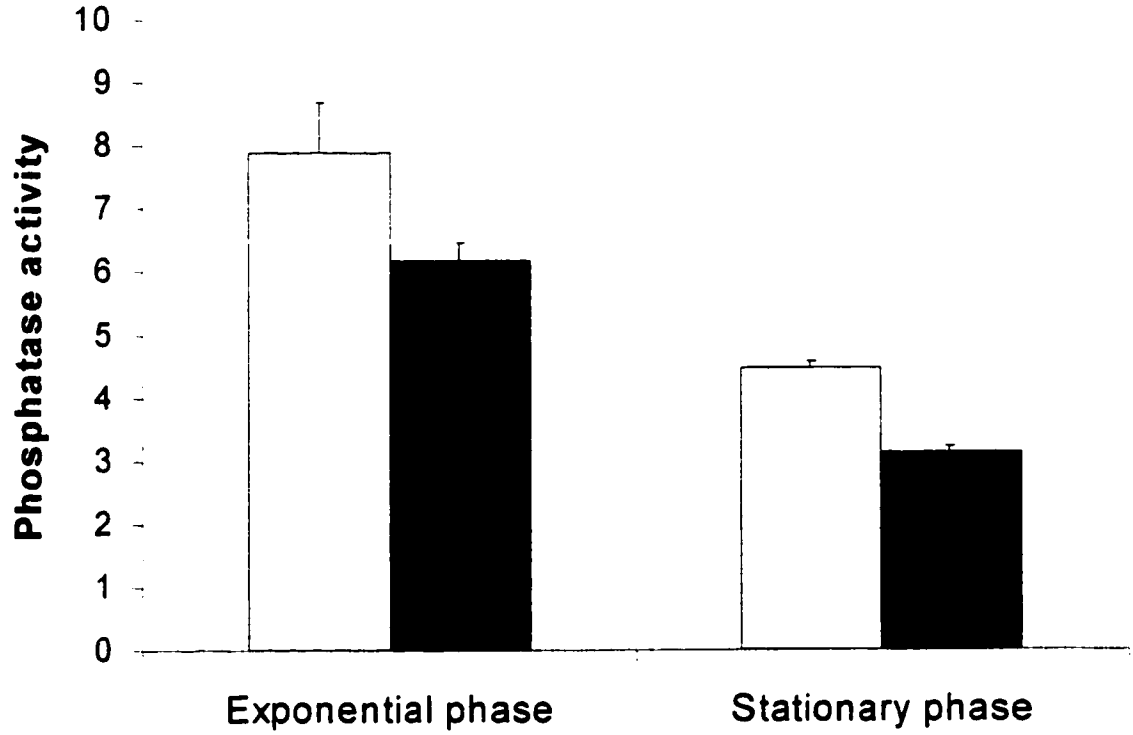

Figure 5.3 Comparison of exponential- and stationary-phase levels of phosphatase activity in Δ*ccp1* (dark bars) and isogenic wild-type cells (white bars). Cells were harvested in exponential- or stationary-phase and lysed with glass beads. Phosphatase activity is reported in units/mg protein where one unit of phosphatase activity is defined as the amount that causes the production of 1 μmol of *p*-nitrophenolate ion/min from the hydrolysis of *p*-nitrophenylphosphate at 22°C. Values are means ± S.D of three experiments.

cells.

The decreased glutathione levels measured in *Δccp1* cells may also be involved in their decreased phosphatase activity. Denu and Tanner have shown that reactivation of H_2O_2-inhibited PTP's is directly correlated to GSH concentrations (73). Therefore, if phosphatases are being inhibited by H_2O_2 in yeast strains, the lower glutathione levels present in the *Δccp1* strain would result in their decreased reactivation, also possibly explaining the results seen in Figure 5.3.

As phosphatases down regulate signals activated by kinases, it is possible that an overactive *ras*-adenylate cyclase pathway (which results in increased PKA activity) might also be due to decreased phosphatase activity. This of course would depend on which phosphatases are being inhibited, and would therefore require more specific testing than the phosphatase assay conducted here.

CHAPTER 6

THE ENGINEERING OF Δ*TSA1* AND Δ*HO* YEAST STRAINS

Introduction

Thioredoxin peroxidase belongs to a family of proteins named the peroxiredoxin (prx) family (31). The fact that prx proteins exist as multiple copies in mammalian cells, and have been discovered in connection with cellular functions such as proliferation, differentiation, osteoregulation, keratinocyte function and natural killer-cell activity, has led to the hypothesis that prx proteins participate in cell signaling by regulating the intracellular concentration of H_2O_2 (31). However, there is no experimental data yet on whether or not H_2O_2 plays a role in cell signaling in *S. cerevisiae*. A role for thioredoxin peroxidase in protection from oxidative stress has, however, been demonstrated in *S. cerevisiae* since *TSA1* mutant strains are sensitive to H_2O_2 as well as oxidative stress induced by heat (46). Furthermore, *TSA1* mutants exhibit slow growth in the presence of H_2O_2, under aerobic conditions (46).

In order to further investigate the role of peroxidases in yeast, a strain deficient in the cytosolic peroxidase, thioredoxin peroxidase, was engineered. This yeast strain was created through a PCR-mediated gene replacement in which the open reading frame (ORF) of *TSA1* was replaced with the *KAN* gene, which encodes resistance to the antibiotic geneticin. A yeast strain deficient in the *HO* gene was also engineered as a control to verify that the insertion of the *KAN* gene does not result in effects that might erroneously be attributed to *TSA1* function. *HO* has no known role, apart from mating type switching, and it has been used as the site of insertion of heterologous genes in

brewing yeasts without any perceptible effect on the fermentation characteristics of the organism (89).

Performing a PCR-based gene replacement in yeast requires three basic steps: (1) amplification of the gene to be inserted in the yeast genome (2) transformation of the yeast with the replacement gene and (3) verification that the replacement gene has been inserted into the right location in the genome. An outline of the steps involved in engineering the *Δho* and *Δtsa1* yeast strains is displayed in Figure 6.1, while the primers used to generate and verify that the desired mutations occurred are displayed in Table 6.1.

The first step in engineering the yeast knockouts is the preparation of the appropriate inserts to be used in the transformations. The *KAN* gene was selected as the replacement gene as it offers protection against geneticin, and thus makes an ideal selection marker. Additionally, as opposed to some nutritional selection markers, it has been shown not to interfere in yeast metabolism (89). In order to replace a desired gene with the *KAN* gene, it is necessary to attach flanking sequences to the *KAN* gene so that the gene to be replaced can be targeted. These 5'- and 3'- flanking sequences are identical to the 5'- and 3'- sequences, respectively, that flank the gene to be replaced in the yeast genome. This enables the *KAN*-containing insert to bind to bases immediately upstream and downstream of the desired gene, positioning the *KAN* module alongside the gene to be replaced; then, through the process of homologous recombination, a small number of yeast cells will replace the targeted gene with the *KAN* gene leading to the desired mutant strain. Cells that undergo transformation are selected based upon their ability to grow on YPD plates containing geneticin, and subjected to a series of PCR reactions to determine if transformation occurred at the correct place in the genome.

Table 6.1 Primers used in construction and verification of *Δtsa1* and *Δho* yeast strains

Oligonucleotide	Sequence	Function
1	5'-CGTCGGGTTTTCTGACAAAT-3'	Amplification of 5'-end of *TSA1* flanking sequence joined to *KAN* gene (coding-strand).
2	5'-TTACGCGTTTTAGAGCCAGA-3'	Amplification of 3'-end of *TSA1* flanking sequence joined to *KAN* gene (antisense-strand).
3	5'-GTGCGCAACCTCATCTCTACA-3'	Verification of *KAN* replacement of *TSA1* at 5'-end. External to *KAN* on the coding-strand.
4	5'-TGTCGCCTAGAAGGGAAATCA-3'	Verification of *KAN* replacement of *TSA1* at 3'-end. External to *KAN* on the antisense-strand.
5	5'-ATATCCTCATAAGCAGCAATCA ATTCTATCTATACTTTAACAGCTGA AGCTTCGTACGC-3'	Amplification of *KAN* at 5'-end (last 19 bases). First 41 bases are homologous to the 5'-region upstream from the start codon in *HO*. (coding-strand).
6	5'-TACTTTTATTACATACAACTTTT TAAACTAATATACACATTTAGGCC ACTAGTGGATCTG-3'	Amplification of *KAN* at 3'-end (last 19 bases). First 41 bases are homologous to the 3'-region downstream the stop codon in *HO* (antisense-strand).
7	5'-TGTTGAAGCATGATGAAGCG-3'	Verification of *KAN* replacement of *HO* at 5'-end. External to *KAN* on the coding-strand.
8	5'-TGGCGTATTTCTACTCCAGCA-3'	Verification of *KAN* replacement of *HO* at 3'-end. External to *KAN* on the antisense-strand.
9	5'-GCAGCGAGGAGCCGT-3'	Verification of *KAN* insertion at 5'-end (antisense-strand internal primer)
10	5'-GATGACGAGCGTAAT-3'	Verification of *KAN* insertion at 3'-end (coding-strand internal primer).

Results and Discussion

Amplification of the KAN Replacement Marker.

As a yeast strain that had already had its *TSA1* gene replaced by *KAN* was available (Steve Veronneau, McGill University), DNA from this *TSA1*:: *KAN* strain was used to create the insert needed to transform the W303-1B strain. Genomic DNA isolated from

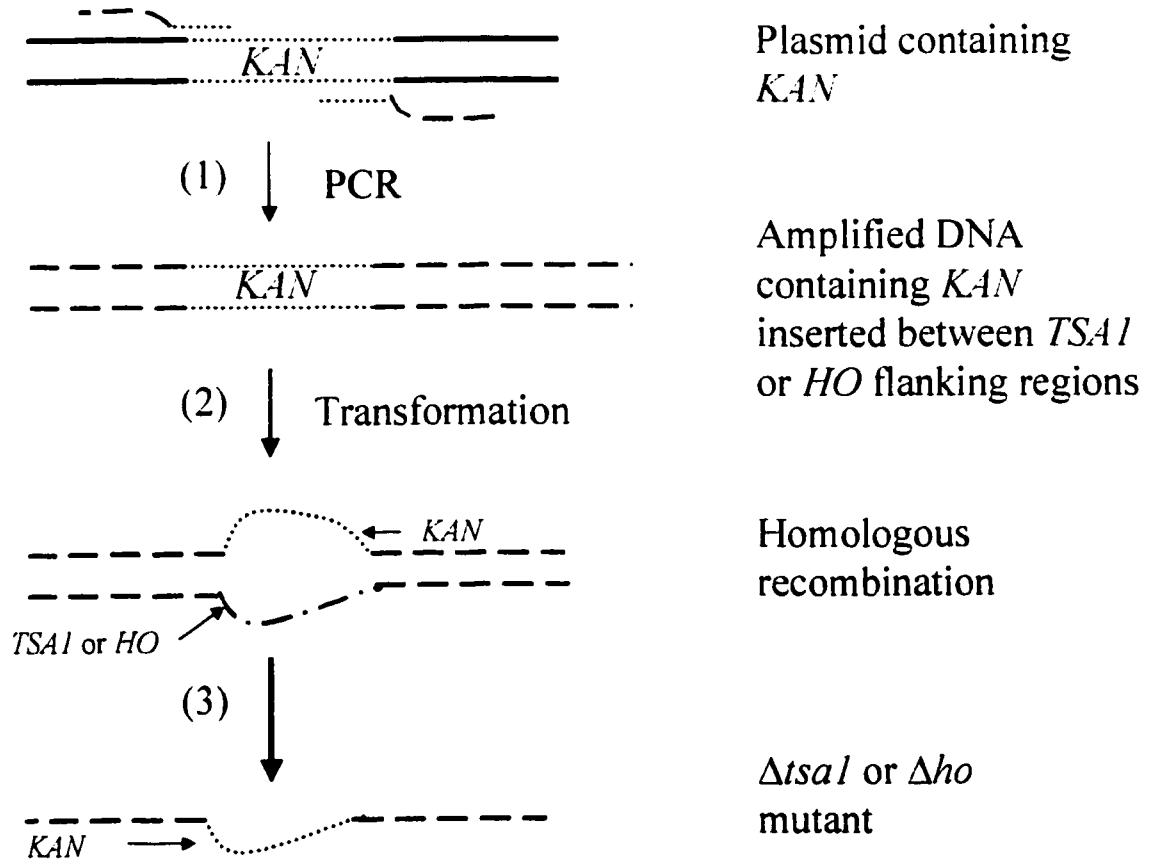

Figure 6.1 Outline of the steps involved in engineering the Δ*tsa1* and Δ*ho* yeast strains. (1) The *KAN* gene (•••) is amplified by primers containing ends that are homologous to the flanking region of the gene to be replaced (——). (2) The PCR product is used to transform wild-type cells. (3) The *TSA1* or *HO* genes (• –) are replaced through a process of homologous recombination.

the *TSA1::KAN* strain using the methods outlined in experimental procedures (Section 2.3), and the *KAN* gene, along with its flanking sequences (192 bases upstream from the start codon and 188 bases downstream of the stop codon), were amplified by PCR using primers 1 and 2 (Table 6.1). As the *KAN* insert is 1550 bases, the resulting oligonucleotide should be 1930 bases and should be readily targeted to the appropriate location in the genome during transformation because of the large flanking regions of sequence identity. The generation of a 1930-base oligonucleotide (fragment 1) was verified by DNA agarose electrophoresis (Figure 6.2A) and this was used for the transformation of W303-1B.

It is desirable to amplify the *KAN* gene and appropriate flanking sequences from a yeast strain already deficient in the gene one wishes to replace. This is because one can generate long flanking sequences that result in easy targeting of the *KAN* gene in the new strain. When amplifying the *KAN* gene from the pFA6-KAN-4 plasmid, the appropriate flanking sequences must be incorporated into the primers used to amplify the *KAN* gene. The flanking sequences are synthesized and incorporated into the primers as noncohesive ends and the *KAN* gene with the desired flanking sequences is amplified by PCR (Figure 6.1)

Because a *HO::KAN* yeast strain was not available, it was necessary to create an oligonucleotide containing the *KAN* gene flanked by sequences identical to the sequences flanking *HO* in the yeast genome. To accomplish this, primers 5 and 6 were used to amplify the *KAN* gene from the pFA6-KAN4 plasmid. The first 41 bases of primer 5 are identical to a region just upstream of the start codon of *HO* (on the coding-strand), and the last 19 bases are identical to the first 19 bases of the *KAN* gene (coding-strand). The

A.

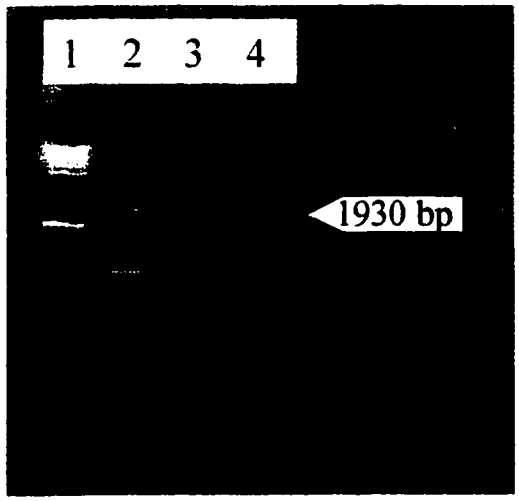

B.

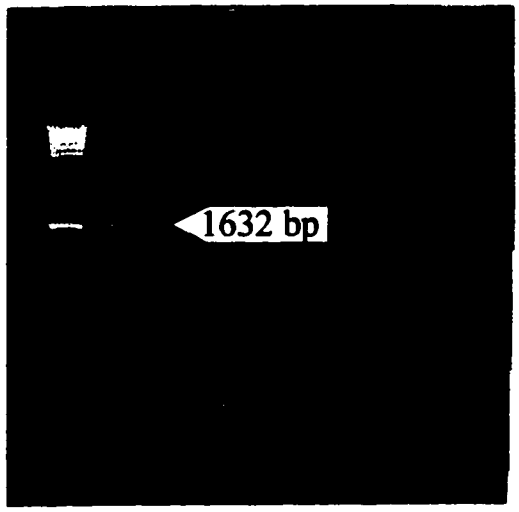

Figure 6.2 Gel analysis of PCR products required to generate (**A**) Δ*tsa1* and (**B**) Δ*ho* yeast strains. (**A**) Lane 1: molecular weight markers. Lane 2: a positive control with wild-type DNA. Lane 4: the desired 1930-base PCR product needed to create a Δ*tsa1* yeast strain (refer to text). (**B**) Lane 1: molecular weight markers. Lane 2: the desired 1632-base PCR product needed to create a Δ*ho* yeast strain (refer to text).

first 41 bases of primer 6 are identical to a region just downstream the stop codon of the *HO* gene (antisense-strand) while the last 19 bases are identical to the last 19 bases of the *KAN* gene (antisense-strand). The result of this PCR reaction is a 1632-base oligonucleotide (1550 + 2 x 41), and formation of this oligonucleotide (fragment 2) was verified by DNA agarose electrophoresis (Figure 6.2B)

Transformation and Recombination

With the successful construction of PCR products containing the *KAN* gene flanked with appropriate targeting sequences, the next step in generating the Δ*tsa* and Δ*ho* yeast strains was the transformation of the yeast cells with fragments 1 and 2 respectively. Yeast cells were transformed with 10-25μl of PCR generated DNA fragments using the lithium acetate method (76) (Section 2.2). Carrier DNA was added to aid in the uptake of fragments 1 and 2 (76). To select for cells that had undergone homologous recombination, aliquots were grown on YPD plates containing approximately 0.03% geneticin and transformants selected after 48 h of growth.

Verification of Proper KAN Insertion

Transformed cells were subjected to a series of PCR reactions to determine if the *KAN* gene had been inserted at the proper location in the genome. To determine whether or not transformation with fragment 1 resulted in the generation of a Δ*tsa1* yeast strain, two PCR reactions were carried out using template DNA from the selected transformants and primers 3, 4, 9 and 10 (Table 6.1). Primer 3 binds to the coding-strand 297 bases upstream of the *TSA1* start codon. Primer 9 binds to the antisense-strand, inside the *KAN*

gene, 274 bases downstream of the start codon. If the *KAN* gene has been properly inserted into the yeast genome, replacing the *TSA1* gene, then amplification of the template DNA with primers 3 and 9 would result in a 571-base pair fragment. This fragment was detected (Figure 6.3A) and therefore confirms the proper insertion of the *KAN* gene at the 5'-end of the *TSA1* ORF. Primers 4 and 10 were used to determine if the *KAN* gene had been properly inserted into the 3'-end of the *TSA1* ORF. Primer 4 binds to the antisense-strand 286 bases downstream of the *TSA1* stop codon. Primer 10 binds the coding-strand, inside the *KAN* gene, 611 bases upstream of the stop codon. A properly inserted *KAN* gene would now generate an 897 base fragment, which was also detected (Figure 6.3A), showing that the *TSA1* gene had been properly replaced by the *KAN* gene at both ends of the *TSA1* ORF and that the transformant was, in fact, a Δ*tsa1* yeast strain.

To determine if the *HO* gene had been properly replaced by *KAN*, the internal *KAN* primers 9 and 10 were used with primers 7 and 8 and DNA from *HO* transformants in the confirmation PCR reactions. Primer 7 binds to the coding-strand 166 bases upstream of the *HO* start codon, so in a PCR reaction with template DNA from *HO* transformants and primer 9, a properly transformed yeast cell should result in the generation of a 440-base PCR fragment. Agarose gel electrophoresis shows that this fragment is generated (Figure 6.3B) and therefore confirms the proper insertion of the *KAN* gene at the 5'-end of the *HO* ORF. The proper insertion of the *KAN* gene at the 3'-end of the *HO* ORF is demonstrated by the generation of the expected 727-base PCR fragment when template DNA from the transformants is amplified with primers 8, which binds to the antisense-strand 96 bases downstream of the *HO* stop codon, and 10.

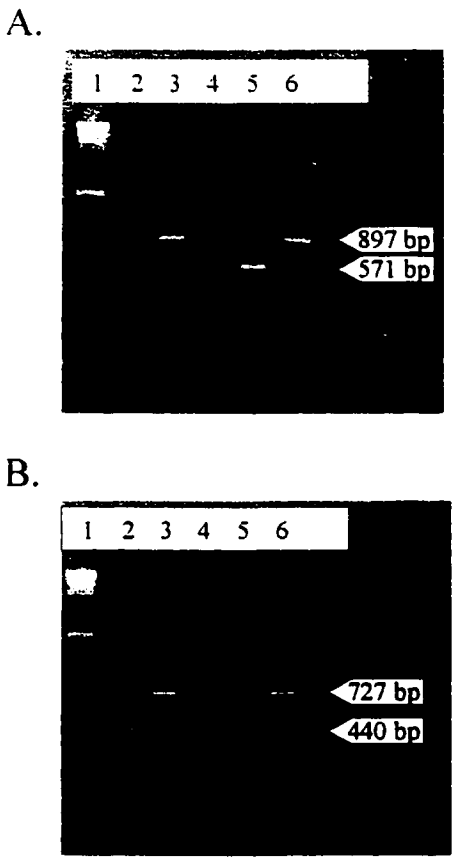

Figure 6.3 PCR confirmation that (**A**) Δ*tsa1* and (**B**) Δ*ho* yeast strains were constructed. Experiments were run in duplicate in each gel. (**A**) Lane 1: molecular weight markers. Lanes 2 and 5: PCR product from Δ*tsa1* transformants confirming the proper insertion of the *KAN* gene into the 5'-end of the *TSA1* ORF. Lanes 3 and 6: PCR product from Δ*tsa1* transformants confirming the proper insertion of the *KAN* gene into the 3'-end of the *TSA1* ORF. (**B**) Lane 1: molecular weight markers. Lanes 2 and 5: PCR product from Δ*ho* transformants confirming the proper insertion of the *KAN* gene into the 5'-end of the *HO* ORF. Lanes 3 and 6: PCR product from Δ*ho* transformants confirming the proper insertion of the KAN gene into the 3'-end of the *HO* ORF.

CHAPTER 7

GENERAL CONCLUSIONS AND SUGGESTIONS FOR FUTURE WORK

General Conclusions

The deletion of the *CCP1* gene from *S. cerevisiae* yields a very interesting strain of yeast that displays (i) altered growth, (ii) decreased mitochondrial function with time, (iii) increased sensitivity to H_2O_2-induced stress and (iv) lowered antioxidant defenses when compared to the isogenic wild-type strain. These properties suggest that CCP functions in protecting mitochondria from time-dependent damage in stationary-phase (most likely due to its ability to eliminate H_2O_2), and also functions in the stationary-phase up regulation of protective mechanisms that eliminate H_2O_2.

The results from Chapter 3, which demonstrate a time-dependent decrease in mitochondrial integrity in Δ*ccp1* cells (Figure 3.5), suggest that CCP functions in protecting mitochondrial enzymes and/or membranes from H_2O_2-induced damage. It appears that in CCP's absence mitochondrial damage to enzymatic or structural components accumulates which, after a few days, severely impairs mitochondrial function. This phenomenon was observed in stationary-phase cells, but mitochondrial damage may well accumulate in growing cells as well. However, it would be difficult to detect mitochondrial damage in these cells since it is continuously diluted out by the production of new healthy cells by cell division. Thus, it seems likely that CCP is required to scavenge endogenous H_2O_2, generated during the process of respiration, that would otherwise lead to mitochondrial inactivation. Peroxynitrite, which is also known to damage cellular components (37) was found by others in our lab to be rapidly reduced by CCP *in vitro*, like H_2O_2 (91). Perhaps the diminished oxygen consumption demonstrated

by the Δ*ccp1* [rho]$^+$ cells (Figure 3.3) is an effort by these cells to stop generation of mitochondrial H_2O_2, which is not quickly eliminated.

The progressive loss of mitochondrial function in the Δ*ccp1* stationary-phase yeast cells might shed some light on processes related to mitochondrial dysfunction in mammalian systems, an event linked with aging, apoptosis and neurodegenerative diseases. Stationary-phase yeast cells are considered to resemble the cells of multicellular organisms in two important aspects: (1) most of their energy comes from mitochondrial respiration and (2) the cells have exited the cell cycle. Damage inflicted on cells that have exited the cell cycle can accumulate and therefore must be prevented or repaired.

In eukaryotes, the production of $O_2^{\bullet-}$ and H_2O_2 in the mitochondria at complexes I and III of the ETC (Figure 1.1) has been convincingly demonstrated in isolated mitochondria or submitochondrial particles exposed to either hypoxia or mitochondrial inhibitors (21). However, few studies in eukaryotes have investigated whether these toxic oxygen species are in fact generated in dangerous concentrations *in vivo*, under physiological conditions (21). Taking advantage of the ability of yeast to survive with non-functional mitochondria, the Δ*ccp1* strain was constructed to provide a good *in vivo* model to test the hypothesis that H_2O_2 generated by the mitochondria under normal metabolic conditions can result in mitochondrial dysfunction if not eliminated. The experiments presented in Chapter 3 suggest that H_2O_2 produced by mitochondria acts directly on mitochondria to cause damage (Figure 3.5), and that H_2O_2 produced *in vivo* induces oxidative damage to mitochondrial components other than mtDNA.

The damage inflicted on the mitochondria in Δ*ccp1* cells might also be due to the decreased activity of other antioxidant enzymes in stationary-phase (Table 5.1), and/or to

Δccp1's decreased glutathione levels. The decreased antioxidant enzyme activity, and the lower glutathione levels displayed by the *Δccp1* yeast strain also likely contribute to the increased susceptibility of *Δccp1* cells to H_2O_2-induced stress during stationary-phase.

The observed coordinated repression in antioxidant activity is consistent with lower activity of the Yap1p transcription factor or increased activity of the *ras*-adenylate cyclase pathway. Intracellular acidification is a known trigger of the *ras*-adenylate cyclase pathway (22), and perhaps an elevated efflux of H_2O_2 from the mitochondria in the absence of CCP, might result in activation of the *ras*-adenylate cyclase pathway. Experiments showing increased PKA activity in *Δccp1* cells (Figure 5.1) reveal that an overactive *ras*-adenylate cyclase pathway is a possibility; however, these experiments can not be considered reliable since they also show stationary-phase levels of PKA to be higher than exponential-phase levels in wild-type yeast, which is a known error (22,50). The fact that the *Δccp1* cells are able to grow on nonfermentable carbon sources (Figure 3.2) is not consistent with an overactive *ras*-adenylate cyclase pathway (Chapter 1, Section 1.5) and suggests that other mechanisms might be involved in decreasing the antioxidant levels.

Although not tested directly, it can be assumed through comparison of *Δccp1* and *Δyap1* yeast strains, that Yap1p levels are reduced in the *Δccp1* cells. How this arises is uncertain, but one possible mediator of Yap1p function is mitochondrial respiration since petite yeast strains are believed to contain lower Yap1p levels (26). Yet mitochondrial respiration was not severely impaired at the time stationary-phase antioxidants were characterized, indicating that mitochondrial respiration is not *directly* responsible for the lower antioxidant levels displayed in *Δccp1* cells. However, perhaps respiration is

involved *indirectly* through generation of H_2O_2. From the experiments in Chapters 3, 4, and 5, it seems that despite being able to grow by respiration, Δ*ccp1* yeast cells do not exert the normal increases in protective mechanisms that accompany respiratory growth. They are more susceptible to stationary-phase challenges of H_2O_2 (Figure 4.2) and do not up regulate catalase and GLR activities to the same extent as isogenic wild-type cells (Table 5.1). A possible explanation for these results is that when cells enter respiratory growth and begin producing H_2O_2, it is sensed by CCP which in turn signals other proteins, possibly through Yap1p, to be up regulated. In this scheme, the H_2O_2 generated from the ETC signals that it is time to initiate the program for long-term survival active during stationary-phase, but requires CCP to do so. If the Δ*ccp1* yeast cells do not undergo all the normal changes involved in stationary phase this might explain this decreased lag time (Figure 3.1). Not having undergone all the changes usually associated with stationary phase, these cells would require less time to leave stationary phase explaining the decreased lag time.

Grant et al. showed that cells given respiratory inhibitors are more susceptible to H_2O_2-induced stress and speculate this increased sensitivity is due to some energy-requiring detoxification process (49). If mitochondria offer protection through such a process, one would expect that the 5-day old Δ*ccp1* cells, with their decreased IRC, would be more susceptible to H_2O_2 challenge than 3-day old cells which contained a higher IRC (Figure 4.3). However the results of Figure 4.3 show this is not the case. The possibility that these cells, over the course of two days, have undergone other changes to offer increased protection seems unlikely as the isogenic wild-type cells do not show any increased protection on day 5 compared to day 3, despite maintaining an IRC of close to

100%. Based on this information it seems likely that changes leading to increased susceptibility to H_2O_2-induced stress have already occurred before day 3 and remain the same throughout days 3 to 5. This further supports the theory that antioxidant defenses are not up regulated upon entry into stationary phase in Δ*ccp1* cells, and suggests that the results reported by Grant et al. could be due to lack of up regulation of protective mechanisms and not energy-driven detoxification.

Despite not increasing antioxidant defenses upon entry into stationary phase, Δ*ccp1* cells appear to be able to up regulate them upon exposure to oxidative stress, as demonstrated by their ability to adapt (Figure 4.4). This suggests that antioxidant defenses are regulated differently upon entry into stationary-phase and upon exposure to exogenous H_2O_2. Whereas small levels of H_2O_2 produced by the respiratory chain might be involved in signaling certain stationary-phase characteristics through CCP, it seems that large levels of exogenous H_2O_2 bypass this step and automatically activate defense mechanisms.

The enzyme activities in exponential-phase cells given in Table 5.1 show that catalase and GLR activities remain almost the same in both Δ*ccp1* and isogenic wild-type cells and suggest, unless glutathione levels are important, that the increased sensitivity of Δ*ccp1* cells to H_2O_2 in this phase is due directly to CCP-mediated H_2O_2 detoxification. The fact that catalase and GLR activities are not altered in exponential-phase Δ*ccp1* cells suggests that CCP is not involved in controlling their activities under these growth conditions. As exponential-phase cells are growing through fermentation and therefore not generating mitochondrial H_2O_2, the exponential-phase activities of catalase and GLR

would fit the above hypothesis for CCP only up regulating catalase and GLR activities when mitochondrial H_2O_2 is present.

The results of the 5.6-fold decrease in exponential-phase glutathione levels is somewhat baffling, especially given that the other antioxidant defense systems appear to have normal levels in this phase (Table 5.1). Decreased Yap1p activity results in only marginally lower glutathione levels (25) and would not account for the 5.6-fold decrease observed in the Δ*ccp1* strain. Tests were carried out to determine if *GSH1* had somehow been disrupted by growing Δ*ccp1* cells in glutathione-free medium. The results suggested that glutathione synthesis was functional and therefore implicate CCP in the reduced glutathione levels seen in Δ*ccp1* cells (data not shown). One possibility is that free glutathione has been consumed in binding to the excess protein radicals present in the Δ*ccp1* strain. If this were the case, this glutathione would not have been detected by the glutathione assay as total protein is precipitated out before glutathione levels are measured. However, given the high activity of other cytosolic peroxidases, this possibility seems unlikely.

Another alternative, which could explain the decreased glutathione levels and antioxidant enzyme activities, is that the cell is trying to commit suicide. It has recently been shown that low levels of H_2O_2 result in apoptosis in yeast, while high levels cause necrosis (40). Evidence that mitochondria are involved in apoptosis in yeast comes from experiments showing that hypoxia prevents H_2O_2-induced apoptosis (40). Mitochondria are known to be pivotal in the induction of apoptosis in mammalian cells and induce apoptosis upon exposure to low levels of H_2O_2 (32). Perhaps when mitochondrial H_2O_2 levels become elevated, yeast cells undergo apoptosis. Although the Δ*ccp1* strain has not

been checked for the typical signs of apoptosis, chromatin condensation and fragmentation, exposition of phosphatidylserine, and the formation of minicells approximating apoptotic bodies, the loss of mitochondrial function and down regulation of other cellular protective mechanisms suggest that *Δccp1* cells may be trying to commit suicide. Apoptosis, unlike necrosis, does not result in membrane permeability (37) and thus apoptotic cell death may not have been detected by vital staining.

Besides being involved in the onset of apoptosis, H_2O_2 in mammalian cells has been shown to be involved in phosphatase inhibition. The finding that removal of *CCP* from *S. cerevisiae* leads to reduced phosphatase activity indicates that yeast might make a good model system to study H_2O_2 signaling, an area of biochemistry currently attracting a lot of attention (31). A yeast strain deficient in thioredoxin peroxidase, which is thought to play a role in controlling H_2O_2 signaling in mammals, has been engineered to further investigate H_2O_2 signaling.

Due to the harm ROS cause there is also a great deal of interest in how proteins involved in the elimination of ROS are controlled. The *Δccp1* yeast strain should serve as a powerful tool to shed light on this topic, as it seems to show alterations in many of the protective mechanisms involved in the elimination of ROS.

Future Work

The present studies on CCP reveal some very interesting insights into the function of this peroxidase in yeast. Equally important, this work raises new questions and highlights opportunities for future work.. The following studies are proposed:

(1) Determine if the mitochondrial damage seen in *Δccp1* cells can be prevented by addition of vitamin E. Since vitamin E has been demonstrated to prevent oxidative damage, it would be interesting to see if *Δccp1* mitochondria could be protected by its addition.

(2) Check *Δccp1* yeast cells for signs of apoptosis. Since these cells most likely have elevated levels of H_2O_2, a characteristic initiator of apoptosis in both mammalian and yeast cells at low levels, it would be interesting to determine if the *Δccp1* cells undergo apoptosis.

(3) Quantify mitochondrial damage in *Δccp1* yeast cells in response to H_2O_2-induced stress. Since metabolically generated H_2O_2 induces mitochondrial damage in *Δccp1* cells (Figure 3.5), it would be interesting to determine if H_2O_2-induced stress also damages *Δccp1* mitochondria.

(4) Determine Yap1p transcriptional activity and Yap1p levels with reporter genes. This would verify the assumption that Yap1p activity is decreased in *Δccp1* cells.

(5) Determine if *Δccp1* yeast cells exhibit other stationary-phase characteristics. This would determine whether or not these cells truly enter stationary-phase or just exit the cell cycle. Since trehalose levels normally increase in stationary phase, one possibility is to examine trehalose content.

(6) Engineer a yeast strain deficient in both the *ccp1* and *CDC25* (the latter would result in constitutively low PKA activity) genes. This would enable one to determine if the phenotype displayed by Δ*ccp1* cells is due to increased PKA activity.

(7) Determine if phosphatase activity is altered in the Δ*tsa1* yeast strain. Since the Δ*ccp1* yeast strain has been shown to possess lower phosphatase activity, it would be worthwhile to determine if thioredoxin peroxidase, known to exist in humans, also affects phosphatase activity, and hence phosphorylation cascades.

(8) Determine if calcium is being released from the mitochondria. Elevated levels of mitochondrial H_2O_2 have been shown to result in mitochondrial Ca^{2+} release in mammals, it may also be occurring in Δ*ccp1* yeast cells. Ca^{2+} is a well known second messenger that can influence growth and gene transcription.

(9) Determine the extent of mtDNA damage. Although structural damage to mitochondrial enzymes and/or membranes is implicated in Δ*ccp1* yeast cells, mtDNA damage, thought to be involved in various pathologies in mammalian cells, was not explored.

REFERENCES

1. Boveris, A. (1976) *Acta Physiol Lat Am* **26**(5), 303-9
2. Altschul, A. M., Abrams, R., and Hogness, T. R. (1940) *J. Biol. Chem.* **136,** 777
3. English, A. M., and Tsaprailis, G. (1995) in *Advances in Inorganic Chemistry* (Skyes, A. G., ed) Vol. 43, pp. 79-125, Academic Press, Inc, California
4. Djavadi-Ohaniance, L., Rudin, Y., and Schatz, G. (1978) *J Biol Chem* **253**(12), 4402-7
5. Yonetani, T. (1970) *Adv Enzymol Relat Areas Mol Biol* **33,** 309-35
6. Goodhew, C. F., Wilson, I. B., Hunter, D. J., and Pettigrew, G. W. (1990) *Biochem J* **271**(3), 707-12
7. Campos, E. G., Hermes-Lima, M., Smith, J. M., and Prichard, R. K. (1999) *Int J Parasitol* **29**(5), 655-62
8. Gonchar, M. V., Kostryk, L. B., and Sibirny, A. A. (1997) *Appl Microbiol Biotechnol* **48**(4), 454-8
9. Williams, P. G., and Stewart, P. R. (1976) *Arch Microbiol* **107**(1), 63-70
10. Verduyn, C., van Wijngaarden, C. J., Scheffers, W. A., and van Dijken, J. P. (1991) *Yeast* **7**(2), 137-46
11. Sels, A. A., and Cocriamont, C. (1968) *Biochem Biophys Res Commun* **32**(2), 192-8
12. Yonetani, T., and Ohnishi, T. (1966) *J Biol Chem* **241**(12), 2983-4
13. Voet, D., and Voet, G. V. J. (1995) *Biochemistry*, Second Ed. (Nedah, R., Ed.), John Wlley & Sons, Inc., Toronto

14. Lee, J., Godon, C., Lagniel, G., Spector, D., Garin, J., Labarre, J., and Toledano, M. B. (1999) *J Biol Chem* **274**(23), 16040-6

15. Izawa, S., Inoue, Y., and Kimura, A. (1996) *Biochem J* **320**(Pt 1), 61-7

16. Verduyn, C., Giuseppin, M. L. F., Scheffers, W. A., and van Dijken, J. P. (1988) *Appl. Environ. Microbiol.* **54**, 2086-2090

17. Davidson, J. F., Whyte, B., Bissinger, P. H., and Schiestl, R. H. (1996) *Proc Natl Acad Sci U S A* **93**(10), 5116-21

18. Kowaltowski, A. J., and Vercesi, A. E. (1999) *Free Radic Biol Med* **26**(3-4), 463-71

19. Darley-Usmar, V. M., Rickwood, D., and Wilson, M. T. (1987) *Mitochondria a practical approach.* The practical approach series, IRL Press Limited, Oxford

20. Chandel, N. S., and Schumacker, P. T. (1999) *FEBS Lett* **454**(3), 173-6

21. Longo, V. D., Liou, L. L., Valentine, J. S., and Gralla, E. B. (1999) *Arch Biochem Biophys* **365**(1), 131-42

22. Thevelein, J. M. (1994) *Yeast* **10**(13), 1753-90

23. Werner-Washburne, M., Braun, E. L., Crawford, M. E., and Peck, V. M. (1996) *Mol Microbiol* **19**(6), 1159-66

24. DeRisi, J. L., Iyer, V. R., and Brown, P. O. (1997) *Science* **278**(5338), 680-6

25. Grant, C. M., Collinson, L. P., Roe, J. H., and Dawes, I. W. (1996) *Mol Microbiol* **21**(1), 171-9

26. Grant, C. M., Maciver, F. H., and Dawes, I. W. (1996) *Mol Microbiol* **22**(4), 739-46

27. Jamieson, D. J. (1992) *J Bacteriol* **174**(20), 6678-81

28. Werner-Washburne, M., Braun, E., Johnston, G. C., and Singer, R. A. (1993) *Microbiol Rev* **57**(2), 383-401

29. Stephen, D. W., Rivers, S. L., and Jamieson, D. J. (1995) *Mol Microbiol* **16**(3), 415-23

30. Flattery-O'Brien, J. A., Grant, C. M., and Dawes, I. W. (1997) *Mol Microbiol* **23**(2), 303-12

31. Rhee, S. G. (1999) *Exp Mol Med* **31**(2), 53-9

32. Kamata, H., and Hirata, H. (1999) *Cell Signal* **11**(1), 1-14

33. Braidot, E., Petrussa, E., Vianello, A., and Macri, F. (1999) *FEBS Lett* **451**(3), 347-50

34. Alberts, B., Bray, D., Lewis, J., Raff, M., Roberts, K., and Watson, J. D. (1994) *Molecular Biology of the Cell*, 3 Ed., Garland Publishing Inc., New York

35. Sandri, G., Panfili, E., and Ernster, L. (1990) *Biochim Biophys Acta* **1035**(3), 300-5

36. Boveris, A., Oshino, N., and Chance, B. (1972) *Biochem J* **128**(3), 617-30

37. Simonian, N. A., and Coyle, J. T. (1996) *Annu Rev Pharmacol Toxicol* **36**, 83-106

38. Moradas-Ferreira, P., Costa, V., Piper, P., and Mager, W. (1996) *Mol Microbiol* **19**(4), 651-8

39. Lenaz, G. (1998) *Biochim Biophys Acta* **1366**(1-2), 53-67

40. Madeo, F., Frohlich, E., Ligr, M., Grey, M., Sigrist, S. J., Wolf, D. H., and Frohlich, K. U. (1999) *J Cell Biol* **145**(4), 757-67

41. Izawa, S., Inoue, Y., and Kimura, A. (1995) *FEBS Lett* **368**(1), 73-6

42. Stephen, D. W., and Jamieson, D. (1996) *FEMS Microbiology Letters* **141**(2-3), 207-212

43. Monteiro, H. P., and Stern, A. (1996) *Free Radic Biol Med* **21**(3), 323-33

44. Longo, V. D., Gralla, E. B., and Valentine, J. S. (1996) *J Biol Chem* **271**(21), 12275-80

45. Godon, C., Lagniel, G., Lee, J., Buhler, J. M., Kieffer, S., Perrot, M., Boucherie, H., Toledano, M. B., and Labarre, J. (1998) *J Biol Chem* **273**(35), 22480-9

46. Hodges, P. E., McKee, A. H. Z., Davis, B. P., Payne, W. E., and Garrels, J. I. (1999) Yeast Proteome Database (YPD): a model for the organization and presentation of genome-wide functional data. *Nucleic Acids Research* **27**, 69-73

47. Chae, H. Z., Kim, I. H., Kim, K., and Rhee, S. G. (1993) *J Biol Chem* **268**(22), 16815-21

48. Chae, H. Z., Chung, S. J., and Rhee, S. G. (1994) *J Biol Chem* **269**(44), 27670-8

49. Grant, C. M., MacIver, F. H., and Dawes, I. W. (1997) *FEBS Lett* **410**(2-3), 219-22

50. Mager, W. H., and De Kruijff, A. J. (1995) *Microbiol Rev* **59**(3), 506-31

51. Bossier, P., Fernandes, L., Rocha, D., and Rodrigues-Pousada, C. (1993) *J Biol Chem* **268**(31), 23640-5

52. Harshman, K. D., Moye-Rowley, W. S., and Parker, C. S. (1988) *Cell* **53**(2), 321-30

53. Moye-Rowley, W. S., Harshman, K. D., and Parker, C. S. (1989) *Genes Dev* **3**(3), 283-92

54. Ransone, L. J., and Verma, I. M. (1990) *Annu Rev Cell Biol* **6**, 539-57

55. Karin, M. (1995) *J Biol Chem* **270**(28), 16483-6

56. Angel, P., and Karin, M. (1991) *Biochim Biophys Acta* **1072**(2-3), 129-57

57. Wu, A. L., and Moye-Rowley, W. S. (1994) *Mol Cell Biol* **14**(9), 5832-9

58. Alarco, A. M., Balan, I., Talibi, D., Mainville, N., and Raymond, M. (1997) *J. Biol Chem* **272**, 19304-13

59. Kuge, S., and Jones, N. (1994) *Embo J* **13**(3), 655-64

60. Wemmie, J. A., Szczypka, M. S., Thiele, D. J., and Moye-Rowley, W. S. (1994) *J Biol Chem* **269**(51), 32592-7

61. Gounalaki, N., and Thireos, G. (1994) *Embo J* **13**(17), 4036-41

62. Amstad, P. A., Krupitza, G., and Cerutti, P. A. (1992) *Cancer Res* **52**(14), 3952-60

63. Devary, Y., Gottlieb, R. A., Lau, L. F., and Karin, M. (1991) *Mol Cell Biol* **11**(5), 2804-11

64. Nose, K., Shibanuma, M., Kikuchi, K., Kageyama, H., Sakiyama, S., and Kuroki, T. (1991) *Eur J Biochem* **201**(1), 99-106

65. Binetruy, B., Smeal, T., and Karin, M. (1991) *Nature* **351**(6322), 122-7

66. Boyle, W. J., Smeal, T., Defize, L. H., Angel, P., Woodgett, J. R., Karin, M., and Hunter, T. (1991) *Cell* **64**(3), 573-84

67. Pulverer, B. J., Kyriakis, J. M., Avruch, J., Nikolakaki, E., and Woodgett, J. R. (1991) *Nature* **353**(6345), 670-4

68. Lin, A., Frost, J., Deng, T., Smeal, T., al-Alawi, N., Kikkawa, U., Hunter, T., Brenner, D., and Karin, M. (1992) *Cell* **70**(5), 777-89

69. Yan, C., Lee, L. H., and Davis, L. I. (1998) *The Embo Journal* **17**, 7416-7429

70. Kuge, S., Jones, N., and Nomoto, A. (1997) *Embo J* **16**(7), 1710-20

71. Fernandes, L., Rodrigues-Pousada, C., and Struhl, K. (1997) *Mol Cell Biol* **17**(12), 6982-93

72. Suzuki, Y. J., Forman, H. J., and Sevanian, A. (1997) *Free Radic Biol Med* **22**(1-2), 269-85

73. Denu, J. M., and Tanner, K. G. (1998) *Biochemistry* **37**(16), 5633-42

74. Denu, J. M., Zhou, G., Guo, Y., and Dixon, J. E. (1995) *Biochemistry* **34**(10), 3396-403

75. Wach, A., Brachat, A., Pohlmann, R., and Philippsen, P. (1994) *Yeast* **10**(13), 1793-808

76. Gietz, and Woods. (1994) *Molecular Genetics of Yeast.* A Practical Approach (Johnston, J. R., Ed.), IRL Press, Oxford, UK

77. Hieda, K., Kobayashi, K., Ito, A., and Ito, T. (1984) *Radiat Res* **98**(1), 74-81

78. Roggenkamp, R., Sahm, H., and Wagner, F. (1974) *FEBS Lett* **41**(2), 283-6

79. Di Ilio, C., Polidoro, G., Arduini, A., Muccini, A., and Federici, G. (1983) *Biochem Med* **29**(2), 143-8

80. Anderson, M. E. (1985) *Methods Enzymol* **113**, 548-55

81. Akerboom, T. P., and Sies, H. (1981) *Methods Enzymol* **77**, 373-82

82. Bradford, M. M. (1976) *Anal Biochem* **72**, 248-54

83. Flattery-O'Brien, J., Collinson, L. P., and Dawes, I. W. (1993) *J Gen Microbiol* **139**(Pt 3), 501-7

84. Klein, C. J., Rasmussen, J. J., Ronnow, B., Olsson, L., and Nielsen, J. (1999) *J Biotechnol* **68**(2-3), 197-212

85. Friis, J., Szablewski, L., Christensen, S. T., Schousboe, P., and Rasmussen, L. (1994) *FEMS Microbiol Lett* **123**(1-2), 33-6

86. Richter, C., Gogvadze, V., Laffranchi, R., Schlapbach, R., Schweizer, M., Suter, M., Walter, P., and Yaffee, M. (1995) *Biochim Biophys Acta* **1271**(1), 67-74

87. Collinson, L. P., and Dawes, I. W. (1992) *J. Gen. Microbiology* **138,** 329-335

88. Chaudhuri, B., Ingavale, S., and Bachhawat, A. K. (1997) *Genetics* **145**(1), 75-83

89. Baganz, F., Hayes, A., Marren, D., Gardner, D. C., and Oliver, S. G. (1997) *Yeast* **13**(16), 1563-73

90. Pitt, A. M., Lee, C. (1996) *Journal of Biomoleular Screening* **1** (1), 47-50

91. Bakas, I. (1999) in *Chemistry and Biochemistry*, Concordia University, Montreal

92. Janssen, K. (1993) in *Current Protocols in Molecular Biology* (K, J., ed) Vol. 2, Greene Publishing Associates, Inc. and John Wiley & Sons, Inc., New York